Tests on the Post-Punching Behavior of Reinforced Concrete Flat Slabs

Essais sur le comportement post-critique des planchers-dalles en béton armé

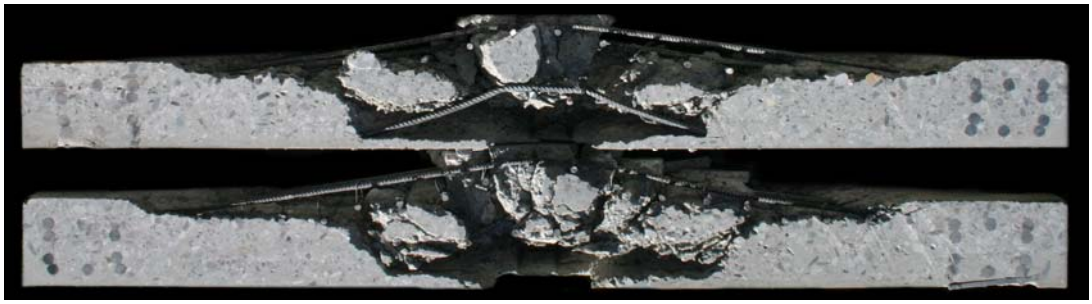

Ecole Polytechnique Fédérale de Lausanne
Institut de Structures
Laboratoire de Construction en Béton

Yaser Mirzaei
Prof. Dr. Aurelio Muttoni

October 2008

This research is funded by the Swiss association of the cement industry (CEMSUISSE)

Table of contents

1 Introduction

This report presents the results of an extensive experimental campaign carried out at the Ecole Polytechnique Fédérale de Lausanne. The post-punching behavior of 24 tested slabs, with 125 mm thickness and various reinforcement layouts are presented and discussed. The performance and robustness of the various solutions is investigated to obtain physical explanations of the load-carrying mechanisms after punching shear failure.

1.1 Scope

Flat plates are a very common and competitive structural system for cast in place slabs in buildings. Using flat slabs as structural elements decreases the time of construction and thus makes it very economical. Due to the highly complex tri-axial state of stress over the columns, brittle punching failure is the major disadvantage of reinforced concrete flat slabs supported by columns. Punching shear failure occurs with almost no warning signs since deflections are small and cracks at the top side of the slab are usually not visible. A local punching failure at one column will result in increased curvatures of the slab at surrounding columns which can trigger the punching failure to the adjacent columns resulting in the progressive collapse of the entire structure. Over the past decades, several collapses due to punching shear failures have occurred resulted in human casualties and large damages showing some shortcomings in the codes of practice as can be seen in Fig. 1.1.

a) Shopping center, Serfontana, Switzerland, 70's

b) Underground parking garage, Bluche, Switzerland, 1981

c) Underground parking garage, Switzerland, 2004

Figure 1.1: Structural collapses due to the punching shear failure

Integrity reinforcement crossing the column and detailed with the intent to provide sufficient post-punching strength can be used to avoid the propagation of punching to adjacent column. To that aim, the Swiss Standard 262 [1] requires that some reinforcement shall be provided on the compression side and be extended over the column and well anchored on both sides (Fig. 1.2 a). Besides this solution, bent-up bars also appear to be a solution to prevent the progressive collapse by providing a ductile behavior [6] (Fig. 1.2 b). This study investigates the post-punching behavior of the various types of integrity reinforcement.

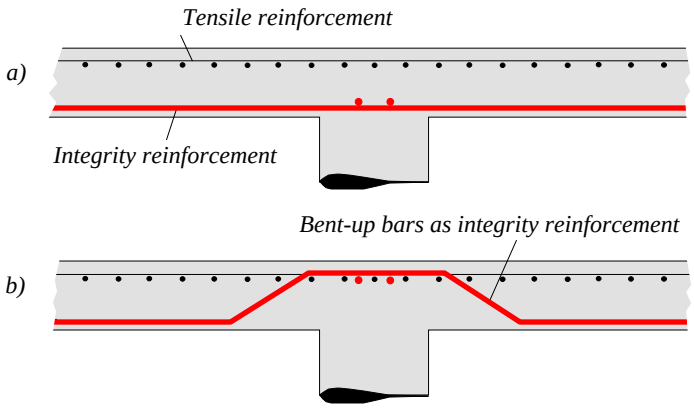

Figure 1.2: Integrity reinforcement: a) Compressive reinforcement and b) Bent-up bars

1.2 Objective

There are main two objectives of this experimental investigation. The first is to study the local behavior of a slab element supported by columns after punching, and to establish a load-deformation relationship as a function of tensile and compressive reinforcement. The second is to investigate the effect of tensile reinforcement, compressive reinforcement and bent-up bars acting as shear reinforcement on the post-punching behavior of flat slabs. This investigation aims at decreasing the vulnerability of the flat slabs to serious accidents while preserving their economic advantages, their simplicity, and at establishing the bases for the design of economic solutions and ease of construction. For that purpose, a mechanical model and applicable constructive details will be developed.

1.3 Acknowledgements

This research was performed at the Concrete Structures Laboratory (IS-BETON) of the Ecole Polytechnique Fédérale de Lausanne, under the supervision of Prof. Dr. Aurelio Muttoni.

The financial support granted by the Swiss Association of the Cement Industry (CEMSUISSE) is deeply appreciated.

The authors would like to thank Dr. Olivier Burdet for the carefully reading the text and proposing valuable suggestions. The authors are also grateful to the technical staff of the Structural Concrete Laboratory of the Ecole Polytechnique Fédérale de Lausanne for their valuable help in this experimental campaign.

2 Description of the slabs

2.1 Overview

Three test series on a total of 24 flat plates were carried out at the Structural Concrete Laboratory of the Ecole Polytechnique Fédérale de Lausanne to investigate the post-punching behavior of flat slabs supported by columns. The first series investigated the effect of tensile reinforcement in the negative moment area over the column on the post-punching behavior of flat slabs. The second series investigated the effect of additional straight bars on the compression side of the slabs and passing through the column and of bent-up bars acting as shear reinforcement. The third series consisted of twelve specimens: four specimens included bent-up bars with a sufficient anchorage length, two specimens included straight compressive reinforcement, two had only tensile reinforcement, and the last four included both tensile reinforcement and straight reinforcing bars passing through the column on the compression side of the slab. The tensile reinforcement was cut-off at specified points to ensure that it did not contribute to the shear transfer after punching failure. In this case, the only link between the punching cone and the rest of the slab is the compressive reinforcement and its influence on the post-punching behavior is investigated. Table 2.1 presents the main parameters and mechanical properties of the specimens. Indices *t* and *c* refer to tensile reinforcement and integrity reinforcement, respectively.

Table 2.1: Reinforcement detail and mechanical properties of materials for all test specimens

			Tensile reinforcement				*Integrity reinforcement*						
	Test	d [mm]	ρ [%]	f_{syt} [MPa]	f_{tt} [MPa]	E_{st} [GPa]	A_{sb}	f_{syc} [MPa]	f_{tc} [MPa]	E_{sc} [GPa]	f_c [MPa]	f_{ct} [MPa]	E_c [GPa]
Series 1	PM-1	102	0.25	601	664	201	-	-	-	-	36.6	2.9	36.9
	PM-2	102	0.49	601	664	201	-	-	-	-	36.5	2.8	36.7
	PM-3	102	0.82	601	664	201	-	-	-	-	37.8	3.4	37.9
	PM-4	102	1.41	601	664	201	-	-	-	-	36.8	3.0	37.1
Series 2	PM-9	102	0.82	601	664	201	4Ø8	616	680	202	31.0	2.3	33.3
	PM-10	102	0.82	601	664	201	4Ø10	560	599	195	31.1	2.3	33.3
	PM-11	102	0.82	601	664	201	4Ø12	548	625	201	32.3	2.5	33.7
	PM-12	102	0.82	601	664	201	4Ø14	527	629	199	32.4	2.6	33.7
	PM-13	102	0.82	601	664	201	4Ø8	616	680	202	32.6	2.6	33.8
	PM-14	102	0.82	601	664	201	4Ø10	560	599	195	32.7	2.6	33.8
	PM-15	100	0.84	601	664	201	4Ø12	548	625	201	32.7	2.6	33.8
	PM-16	101	0.83	601	664	201	4Ø14	527	629	199	32.8	2.6	33.9
Series 3	PM-17	102	0.82	625	641	200	4Ø8	625	641	200	39.7	2.8	28.7
	PM-18	95	0.88	625	641	200	4Ø10	605	658	194	39.8	2.8	28.8
	PM-19	99	0.85	625	641	200	4Ø12	559	618	197	39.9	2.8	28.8
	PM-20	102	0.82	625	641	200	4Ø14	578	695	203	40.0	2.9	29.0
	PM-21	103	0.81	625	641	200	4Ø8	625	641	200	40.2	2.9	29.3
	PM-22	99	0.85	625	641	200	4Ø10	605	658	194	40.3	2.9	29.5
	PM-23	95	0.88	625	641	200	-	-	-	-	40.4	2.9	29.7
	PM-24	97	0.86	625	641	200	-	-	-	-	40.4	3.0	29.9
	PM-25	98	0.85	625	641	200	4Ø8	625	641	200	40.4	3.0	30.1
	PM-26	101	0.83	625	641	200	4Ø10	605	658	194	40.3	3.0	30.1
	PM-27	104	0.81	625	641	200	4Ø12	559	618	197	40.3	3.0	30.2
	PM-28	99	0.85	625	641	200	4Ø14	578	695	203	40.3	3.0	30.3

2.2 Geometry and reinforcement

The twenty four square slab elements tested in this experimental program were identical in size and shape. The total width of the slabs was 1500 mm and nominal total thickness of the slabs was 125 mm. The square steel plate of 130 x 130 mm was used to simulate a rigid column in all tests. Fig. 2.1 shows the general dimensions and geometry of the slabs.

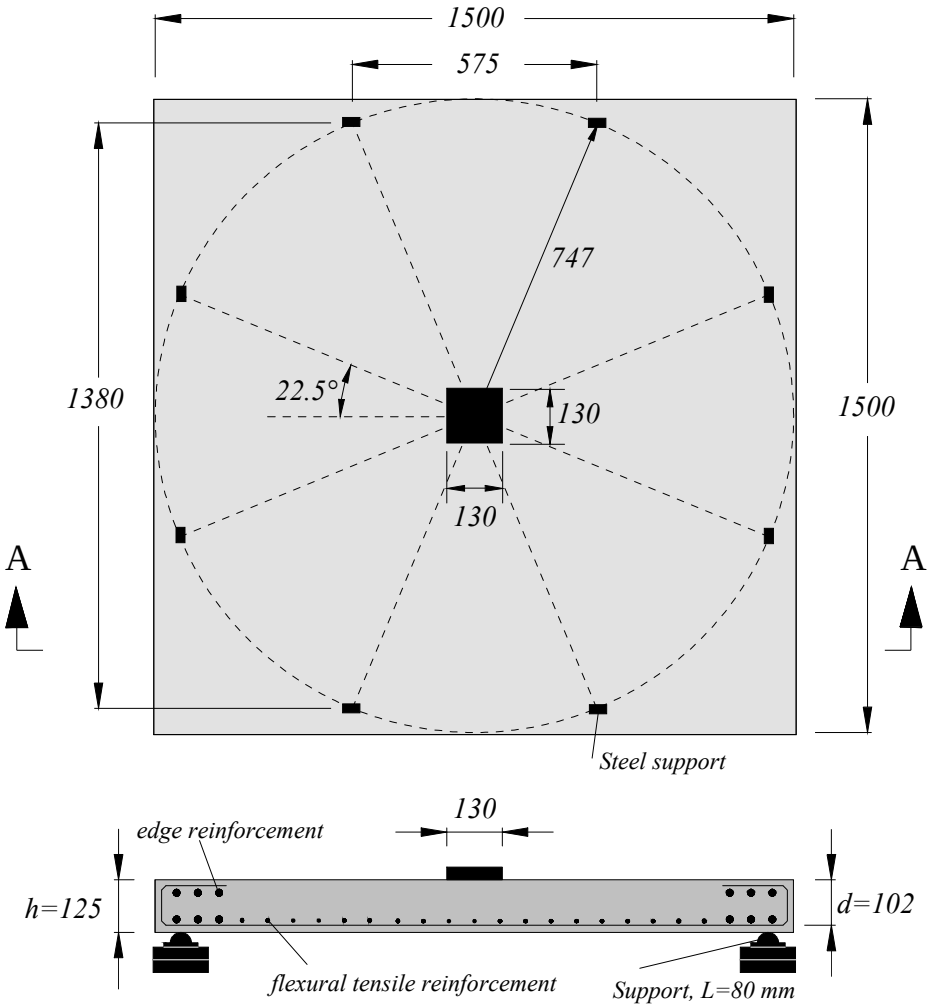

Figure 2.1: Typical slab dimensions, plan and section [mm]

For all specimens, Ø8 was used as the main diameter for the tensile reinforcement. The first four specimens, PM-1 to PM-4, were designed to investigate the effect of various reinforcement ratios on the post-punching behavior of flat slabs. The variation of the reinforcement ratio was achieved by changing the bar spacing, see Fig. 2.2. For the remaining twenty specimens, the tensile reinforcement ratio was the same and equal to 0.82% (Ø8 at 60 mm). For all slabs, the nominal concrete cover was 15 mm and Ø8 was used as the main tensile reinforcing bar, therefore the nominal effective depth (the average effective distance from the extreme compression fiber to the centroid of the tensile reinforcing bars) was 102 mm. The simulated column consisted of a stack of three square steel plates with the dimension of 130 x 130 x 30 mm. No vertical shear reinforcement was provided.

As can be seen in Fig. 2.2.e, for slabs PM-9, PM-10, PM-11 and PM-12, Ø8, Ø10, Ø12 and Ø14 were used as integrity reinforcement in the compression zone of the slab. The full anchorage condition for this reinforcement (50Ø for Ø14, according to the SIA 262) was provided, and thus the results should not be influenced by the anchorage condition.

Fig. 2.2 f shows that for slabs PM-13, PM-14, PM-15 and PM-16, Ø8, Ø10, Ø12 and Ø14 bent-up bars were used as integrity reinforcement with an angle of inclination of 30° and bent at a distance of 50 mm from the column face. In addition, with these specimens, the full anchorage length for the bent-up bars was not provided, thus the results were influenced by the anchorage condition.

Fig. 2.3.a shows slabs PM-17, PM-18, PM-19 and PM-20 in which Ø8, Ø10, Ø12 and Ø14 bent-up bars were used as integrity reinforcement respectively. In these tests, the full anchorage length for bent-up bars was provided; in consequence, the results were not affected by the anchorage condition.

PM-21 and PM-22 were similar to PM-9 and PM-10 respectively. PM-23 and PM-24 were similar to PM-3 as well, see Fig. 2.3.b. This series of tests was about to investigate the influence of using various types of reinforcing steel and the effect of the concrete confinement over the column on the post-punching behavior of concrete slab-column connection. It should be noted that cold-work Ø8 as well as hot-rolled Ø14 were used for all tested slabs. For slab PM-22 hot-rolled Ø10 was used and cold-work Ø10 was used for the other test specimens. For slabs PM-11 and PM-15 hot-rolled Ø12 was used and cold-work Ø12 was used for the other test specimens.

Fig. 2.3.c to Fig. 2.3.f show reinforcement layouts for slabs PM-25, PM-26, PM-27 and PM-28. They had Ø8 at 60 mm as their tensile reinforcement. Their tensile reinforcement was cut off at some specified points to investigate the effect of short anchorage length of tensile reinforcement on the post-punching behavior of flat slabs: PM-25 (cut-off at *2d* from the column face); PM-26 (cut-off at *2.5d* from the column face); PM-27 (cut-off at *3d* from the column face); PM-28 (cut-off at *3.5d* from the column face). In addition, Ø8, Ø10, Ø12 and Ø14 were used as integrity reinforcement in the compression zone of the slabs PM-25 to PM-28, respectively.

In all specimens, very strong edge reinforcement in both the top and bottom layer was provided to avoid unexpected modes of failure.

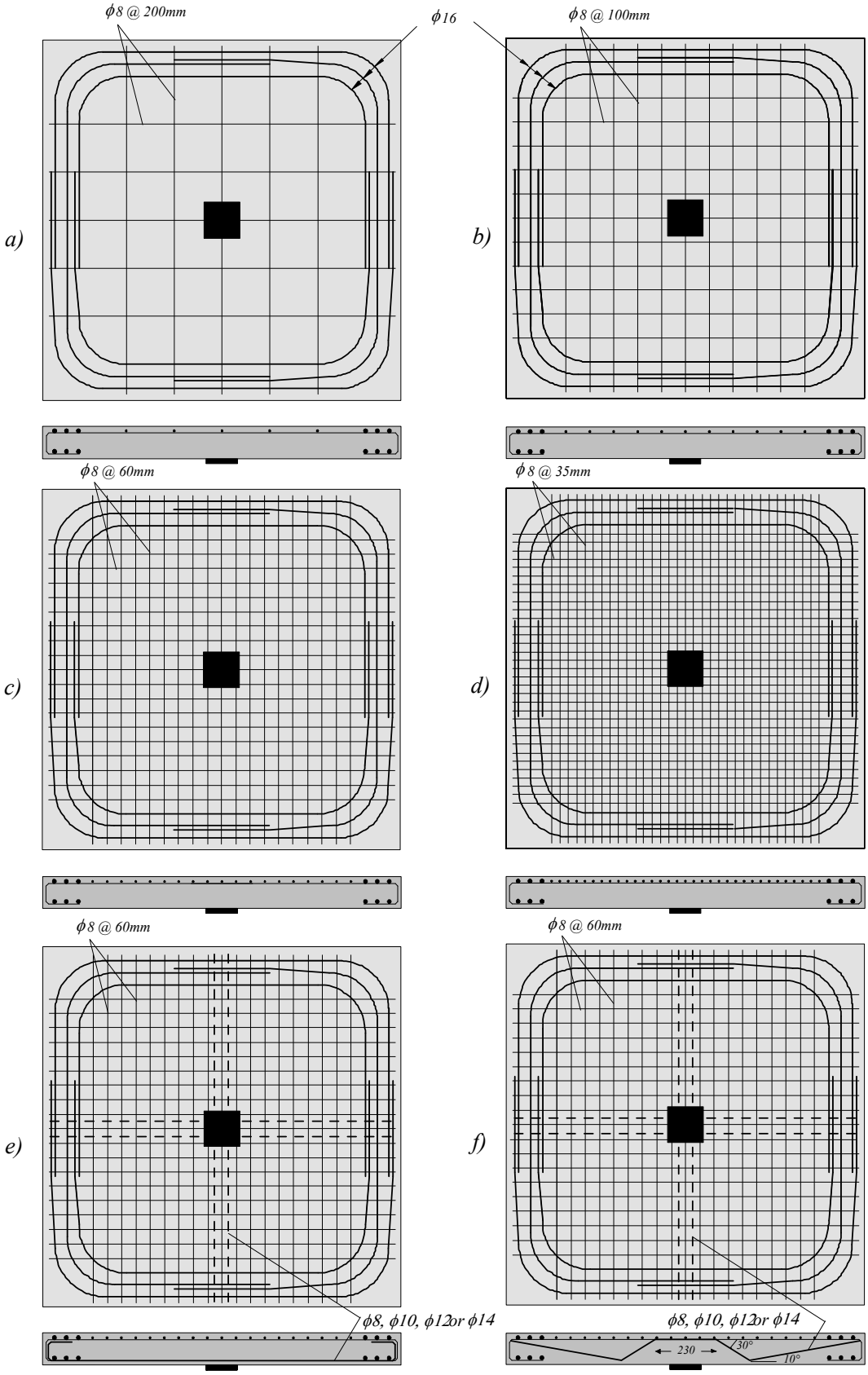

Figure 2.2: Reinforcement layout: a) PM-1, b) PM-2, c) PM-3 and PM-23 d) PM-4, e) PM-9 to PM-12 (ϕ8, ϕ10, ϕ12 and ϕ14), f) PM-13 to PM-16 (ϕ8, ϕ10, ϕ12 and ϕ14)

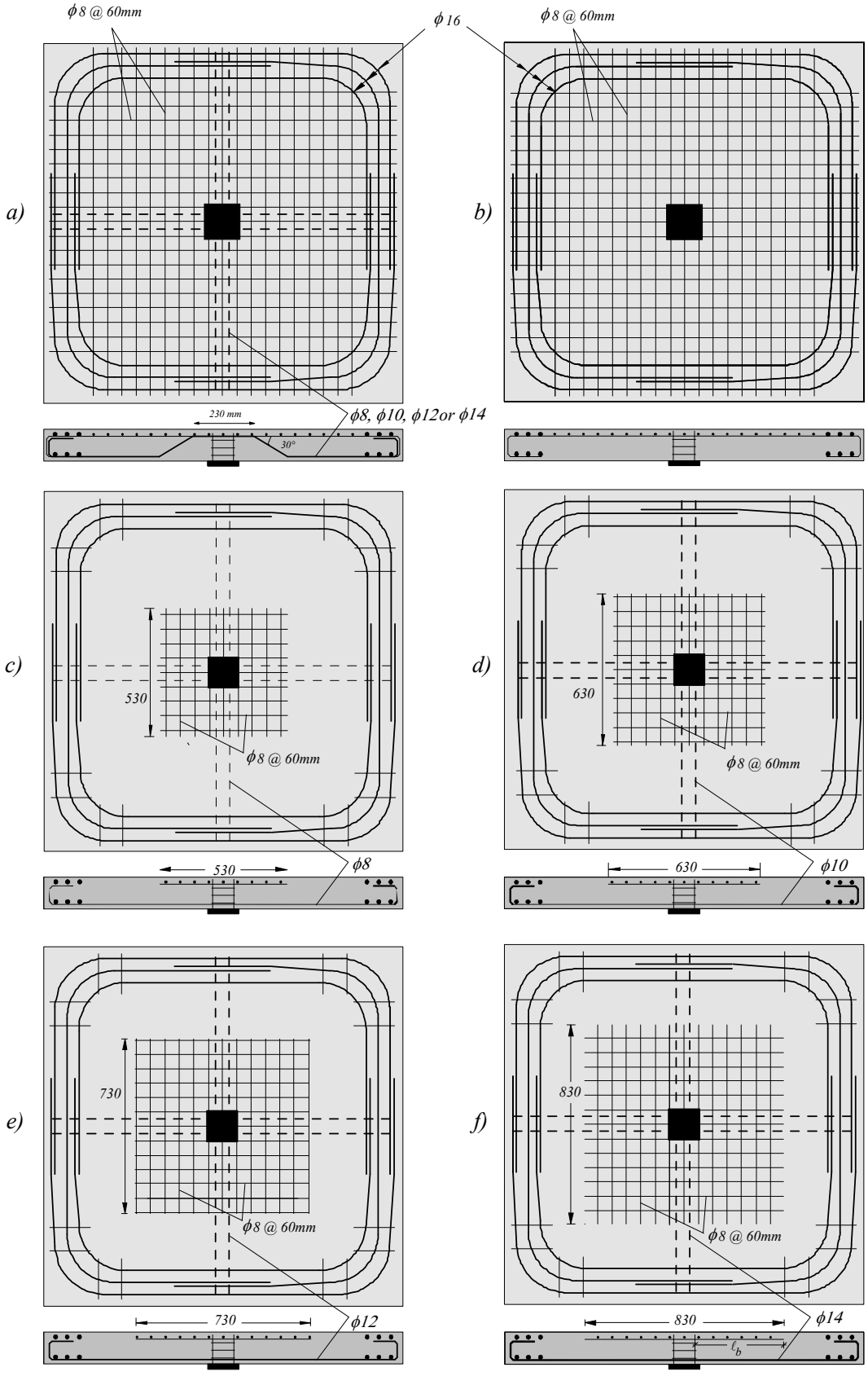

Figure 2.3: Reinforcement layout: a) PM-17 to PM-20 (ϕ8, ϕ10, ϕ12 and ϕ14), b) PM-24, c) PM-25, d) PM-26, e) PM-27, f) PM-28

2.3 Concrete casting and slab preparation

The first and two series were cast at the Laboratory of Structures of the Ecole Polytechnique Fédérale de Lausanne, while the third series was cast by GENETTI, a company located in Riddes,Valais, Switzerland.

Fig. 2.4 shows the main steps of casting and preparation of the slabs. The formwork surface in contact with concrete was impregnated with mould oil before putting in the reinforcement. The concrete was prepared in a batching plant and delivered to the Laboratory of Structures by a concrete mixer truck. The first series was cast on 31st March, 2006, the second on 26th June, 2006 and the last one on 14th May, 2007. The slab surface was levelled and smoothed with the help of a ruler and a mason's mortar board. After casting, the slab was covered with a plastic sheet to maintain a moist environment. Water was sprayed onto the slab during the period of curing. The slump and flow table tests were performed before the casting of the slab. Table 2.2 shows the results of the slump and flow table tests. Three concrete cylinders were cast and tested for each slab using the same batch of concrete.

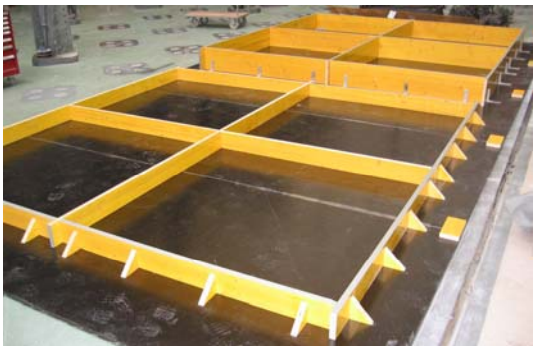

a) Formwork

b) Formwork and reinforcement

c) Dowel steel reinforcing bars

d) Bent-up bars

Figure 2.4: Formwork and reinforcing bars

2.4 Material properties

2.4.1 Concrete

Concrete of type C30/37 was chosen as it is representative for slabs cast in Switzerland. The concrete for the first and the second series was provided by Bétonfrais + pompages SA Company, while for the third series, concrete was provided by GENETTI. The composition of concrete used for the slabs is shown in Table 2.2. The water-cement ratio was about 0.54 for the first two series and 0.49 for the last one. The maximum aggregate size was 16 mm in all test series.

a) Concrete casting

b) Slump test

c) Flow table test

d) Cylinders

e) Slabs PM-9 to PM-16

f) Slabs PM-17 to PM-28

Figure 2.5: Casting of the slabs

The measured mechanical properties were the concrete compressive strength, the Young's modulus, the apparent density and the tensile strength of the concrete. For this purpose, three cylinders were cast using the same concrete for each slab. Each concrete cylinder had a diameter of 160 mm and height of 320 mm. The tests were performed at the Laboratoire de Matériaux de Construction (LMC) of the Ecole Polytechnique Fédérale de Lausanne.

The mechanical properties at the time of testing were measured individually or calculated using the following fitted equations of logarithmic form proposed by CEB-FIP Model Code 90 [14]:

$$f_c(t) = f_{c,28} \exp\{s(1 - \sqrt{\frac{28}{t}})\} \tag{2.1}$$

where s is assumed to be 0.2.

Table 2.2: Concrete composition and results of tests on fresh concrete

Slab	Sand 0-4 [kg]	Gravel 4-8 [kg]	Gravel 8-16 [kg]	Cement [kg]	Water [kg]	Slump [mm]	Flow table test [mm]
Series 1 & 2	753 30%	604 24%	661 26%	325	174 W/C = 0.54	15	350
Series 3	820 35%	432 18%	621 26%	325	159 W/C = 0.54	12	320

Table 2.3: Main concrete properties for the tested slabs

	Test	Date	age	Compressive Strength		Tensile Strength	Young's Modulus	Density
			[day]	$f_{c,28}$	f_c [MPa]	f_{ct} [MPa]	E_c [GPa]	[t/m^3]
Series 1	PM-1	05.05.2006	33	36	36.6	2.9	36.9	2.45
	PM-2	02.05.2006	30	36	36.5	2.8	36.7	2.45
	PM-3	12.06.2006	71	36	39.5	3.4	37.9	2.45
	PM-4	10.05.2006	38	36	36.8	3.0	37.1	2.44
Series 2	PM-9	31.08.2006	35	30	31.0	2.3	33.3	2.42
	PM-10	01.09.2006	37	30	31.1	2.3	33.3	2.42
	PM-11	20.09.2006	56	30	32.3	2.5	33.7	2.41
	PM-12	22.09.2006	58	30	32.4	2.6	33.7	2.42
	PM-13	26.09.2006	62	30	32.6	2.6	33.8	2.42
	PM-14	28.09.2006	64	30	32.7	2.6	33.8	2.42
	PM-15	29.09.2006	65	30	32.7	2.6	33.8	2.42
	PM-16	02.10.2006	68	30	32.8	2.6	33.9	2.41
Series 3	PM-17	18.06.2007	35	37	39.7	2.8	28.7	2.42
	PM-18	19.06.2007	36	37	39.8	2.8	28.8	2.42
	PM-19	20.06.2007	37	37	39.9	2.8	28.8	2.43
	PM-20	22.06.2007	39	37	40.0	2.9	29.0	2.43
	PM-21	26.06.2007	43	37	40.2	2.9	29.3	2.40
	PM-22	29.06.2007	46	37	40.3	2.9	29.5	2.41
	PM-23	03.07.2007	50	37	40.4	2.9	29.7	2.44
	PM-24	06.07.2007	53	37	40.4	3.0	29.9	2.41
	PM-25	09.07.2007	56	37	40.4	3.0	30.1	2.41
	PM-26	10.07.2007	57	37	40.3	3.0	30.1	2.41
	PM-27	11.07.2007	58	37	40.3	3.0	30.2	2.42
	PM-28	13.07.2007	60	37	40.3	3.0	30.3	2.42

Table 2.3 presents the average value of the mechanical properties at the time of failure. Tables 2.4, 2.5 and 2.6 show the results of tests on concrete cylinders for series 1, 2 and 3 respectively. Fig. 2.5 shows the evolution over time of concrete compressive strength, tensile strength and the modulus of elasticity. Fig. 2.6 shows the stress-strain curve in compression for concrete for the first series.

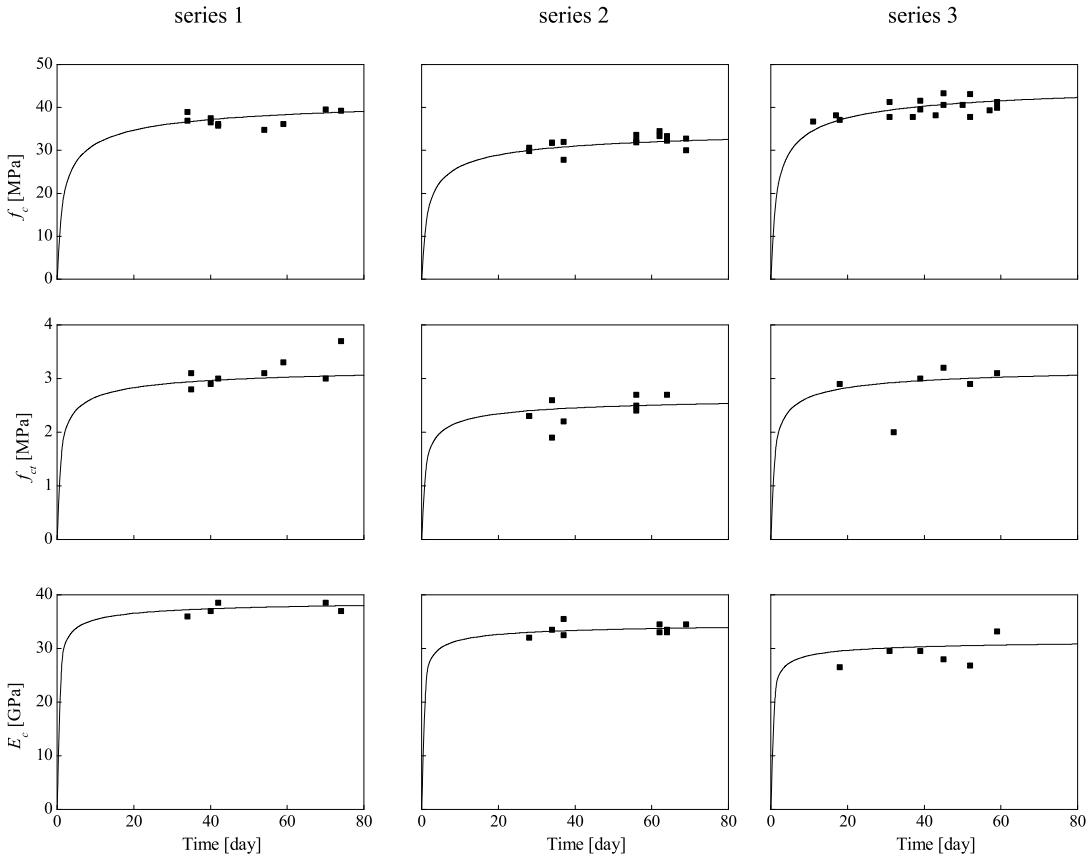

Figure 2.5: Evolution of mechanical properties of concrete over time

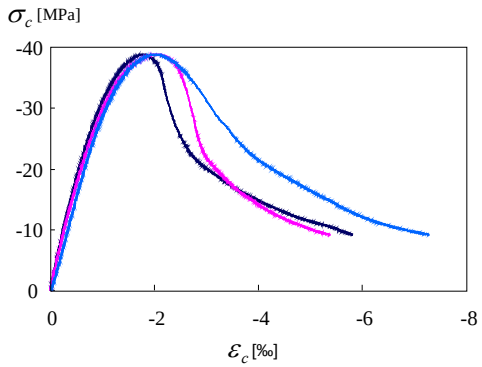

Figure 2.6: Stress-strain curve of concrete in compression

Table 2.4: Results of tests on concrete cylinders for the first series (PM-1 to PM-4)

Date of test	Age	Compressive Strength f_c [MPa]	Tensile Strength f_{ct} [MPa]	Young's Modulus E_c [GPa]	Density [t/m^3]
04.05.2006	34	39.0	-	36.0	2.45
04.05.2006	34	36.9	-	-	2.45
05.05.2006	35	-	3.1	-	2.44
05.05.2006	35	-	2.8	-	2.44
10.05.2006	40	37.5	2.9	37.0	2.44
10.05.2006	40	36.5	-	-	2.44
12.05.2006	42	36.1	3.0	38.5	2.45
12.05.2006	42	35.8	-	-	2.45
24.05.2006	54	34.8	3.1	-	2.44
29.05.2006	59	36.1	3.3	-	2.45
09.06.2006	70	39.5	3.0	38.5	2.44
09.06.2006	70	39.5	3.0	38.5	2.44
13.06.2006	74	39.2	3.7	37.0	2.44
13.06.2006	74	39.2	3.7	37.0	2.44

Table 2.5: Results of tests on concrete cylinders for the second series (PM-9 to PM-16)

Date of test	Age	Compressive Strength f_c [MPa]	Tensile Strength f_{ct} [MPa]	Young's Modulus E_c [GPa]	Density [t/m^3]
23.08.2006	28	30.6	2.3	32	2.42
23.08.2006	28	29.8	-	-	2.42
29.08.2006	34	31.8	1.9	33.5	2.42
29.08.2006	34	31.8	-	-	2.42
01.09.2006	37	32	2.2	32.5	2.42
01.09.2006	37	27.8	-	-	2.42
20.09.2006	56	33.6	-	35.5	2.42
20.09.2006	56	31.9	-	33	2.41
20.09.2006	56	32.4	-	33	2.41
22.09.2006	58	-	2.5	-	2.42
22.09.2006	58	-	2.4	-	2.41
22.09.2006	58	-	2.3	-	2.42
26.09.2006	62	33.3	-	34.5	2.42
26.09.2006	62	34.5	-	-	2.42
27.09.2006	63	-	2.7	-	2.42
28.09.2006	64	33.3	2.7	33.5	2.42
28.09.2006	64	32.3	-	-	2.42
03.10.2006	69	32.8	-	34.5	2.41
03.10.2006	69	30	-	-	2.41
04.10.2006	70	-	2.6	-	2.41

Table 2.6: Results of tests on concrete cylinders for the third series (PM-17 to PM-28)

Date of test	Age	Compressive Strength f_c [MPa]	Tensile Strength f_{ct} [MPa]	Young's Modulus E_c [GPa]	Density [t/m^3]
25.05.2007	11	36.7	-	-	2.44
31.05.2007	17	38.2	-	-	2.42
01.06.2007	18	37.1	2.9	26.5	2.43
14.06.2007	31	37.8	-	29.5	2.43
14.06.2007	31	41.3	-	-	2.43
15.06.2007	32	-	2	-	2.41
20.06.2007	37	37.8	-	-	2.42
22.06.2007	39	39.5	3	29.5	2.43
22.06.2007	39	41.6	-	-	2.43
26.06.2007	43	38.2	-	-	2.40
28.06.2007	45	43.3	3.2	28	2.41
28.06.2007	45	40.6	-	-	2.41
03.07.2007	50	40.6	-	-	2.44
05.07.2007	52	43.1	2.9	26.8	2.41
05.07.2007	52	37.8	-	-	2.41
10.07.2007	57	39.3	-	-	2.41
12.07.2007	59	41.3	3.1	33.2	2.42
12.07.2007	59	39.9	-	-	2.42

2.4.2 Steel

Fig. 2.8 shows the stress-strain relationship for the reinforcing bars used for these test series. All of the reinforcing bars were of the type of B500B according to the Swiss concrete construction code SIA 262 (2003). Table 2.7 presents the average value of the mechanical properties of tensile reinforcement as well as integrity reinforcement for all of the tested slabs. Table 2.8 shows the detailed results for each tensile test. The strains were measured using an extensometer at the centre of the specimen with a measurement length of 100 mm. The loading speed was 10 MPa/s and ℓ is the length of the reinforcement measured between the clamps of the tension testing machine.

Table 2.7: Average mechanical properties of the reinforcement

Test	ϕ_t [mm]	f_{syt} [MPa]	f_{tt} [MPa]	ε_{uc} [%]	E_{sc} [GPa]	ϕ_c [mm]	f_{syc} [MPa]	f_{tc} [MPa]	ε_{uc} [%]	E_{sc} [GPa]
PM-1	8	601	664	7.39	201	-	-	-	-	-
PM-2	8	601	664	7.39	201	-	-	-	-	-
PM-3	8	601	664	7.39	201	-	-	-	-	-
PM-4	8	601	664	7.39	201	-	-	-	-	-
PM-9	8	601	664	7.39	201	8	616	680	7.39	202
PM-10	8	601	664	7.39	201	10	560	599	7.91	195
PM-11	8	601	664	7.39	201	12	548	625	10.46	201
PM-12	8	601	664	7.39	201	14	527	629	13.52	199
PM-13	8	601	664	7.39	201	8	616	680	7.39	202
PM-14	8	601	664	7.39	201	10	560	599	7.91	195
PM-15	8	601	664	7.39	201	12	548	625	10.46	201
PM-16	8	601	664	7.39	201	14	527	629	13.52	199
PM-17	8	625	641	6.07	200	8	625	641	6.07	200
PM-18	8	625	641	6.07	200	10	605	658	7.81	194
PM-19	8	625	641	6.07	200	12	559	618	7.86	197
PM-20	8	625	641	6.07	200	14	578	695	11.97	203
PM-21	8	625	641	6.07	200	8	625	641	8.91	200
PM-22	8	625	641	6.07	200	10	605	658	10.30	194
PM-23	8	625	641	6.07	200	-	-	-	-	-
PM-24	8	625	641	6.07	200	-	-	-	-	-
PM-25	8	625	641	6.07	200	8	625	641	6.07	200
PM-26	8	625	641	6.07	200	10	605	658	7.81	194
PM-27	8	625	641	6.07	200	12	559	618	7.86	197
PM-28	8	625	641	6.07	200	14	578	695	11.97	203

Table 2.8: Detailed results of tests on the reinforcement

Test series	ϕ [mm]	f_y [MPa]	f_t [MPa]	ε_u [%]	f_t/f_y	E_s [GPa]	ℓ [mm]
1,2	8	633	691	7.68	1.09	200	634
1,2	8	581	641	-	1.10	198	601
1,2	8	594	657	-	1.11	202	641
1,2	8	598	668	7.10	1.12	204	652
1,2	10	561	584	5.21	1.04	195	578
1,2	10	555	619	8.68	1.12	195	579
1,2	10	566	585	5.19	1.03	194	584
1,2	10	557	608	5.47	1.09	197	592
1,2	12	556	616	7.01	1.11	195	541
1,2	12	539	633	13.90	1.17	207	592
1,2	14	531	630	14.57	1.19	201	550
1,2	14	523	627	12.46	1.20	196	557
3	8	619	635	6.68	1.03	199	620
3	8	633	651	-	1.03	201	621
3	8	623	637	5.46	1.02	200	627
3	10	619	665	5.41	1.07	191	613
3	10	627	673	5.16	1.07	197	622
3	10	596	642	10.72	1.08	192	605
3	10	579	653	9.88	1.13	194	628
3	12	541	600	7.84	1.11	193	664
3	12	576	632	8.43	1.10	199	649
3	12	581	639	8.75	1.10	194	652
3	12	539	601	6.41	1.12	200	659
3	14	578	697	11.96	1.21	200	674
3	14	583	697	12.23	1.20	206	684
3	14	573	690	11.73	1.20	202	701

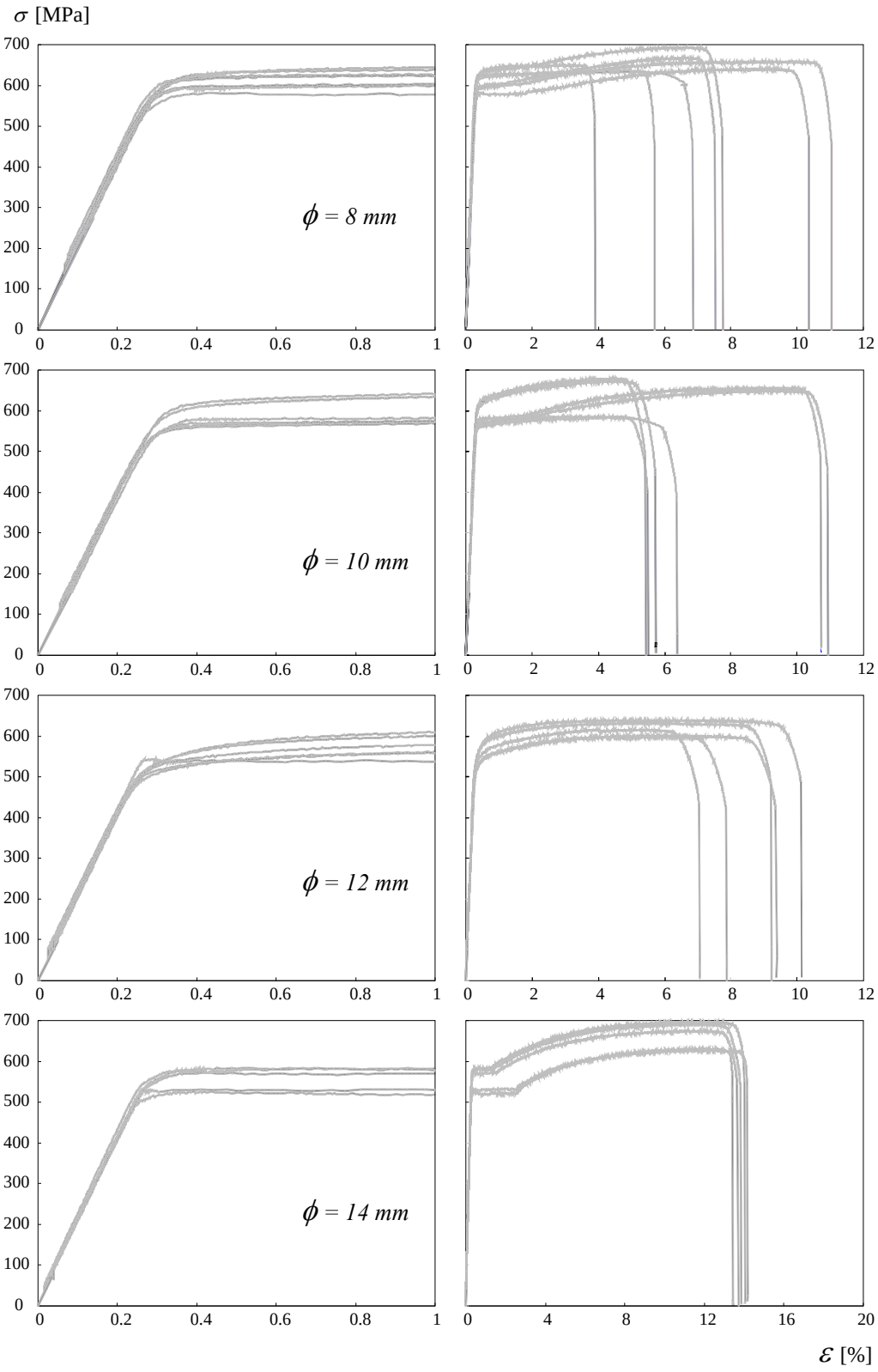

Figure 2.8: Stress-strain curves for steel bars

3 Test setup and instrumentation

3.1 Framework and loading procedure

Fig. 3.1 shows the test setup and the main dimensions of a typical tested slab. The test frame is mainly composed of two principal columns, a strong girder, a hydraulic jack, a load cell, four concrete blocks, steel plates, and also measurement instruments. The columns were fixed to the reaction floor by pre-stressing bars to ensure an adequate rigidity in the system. The load cell and the hydraulic jack were connected to the girder by a steel transfer beam.

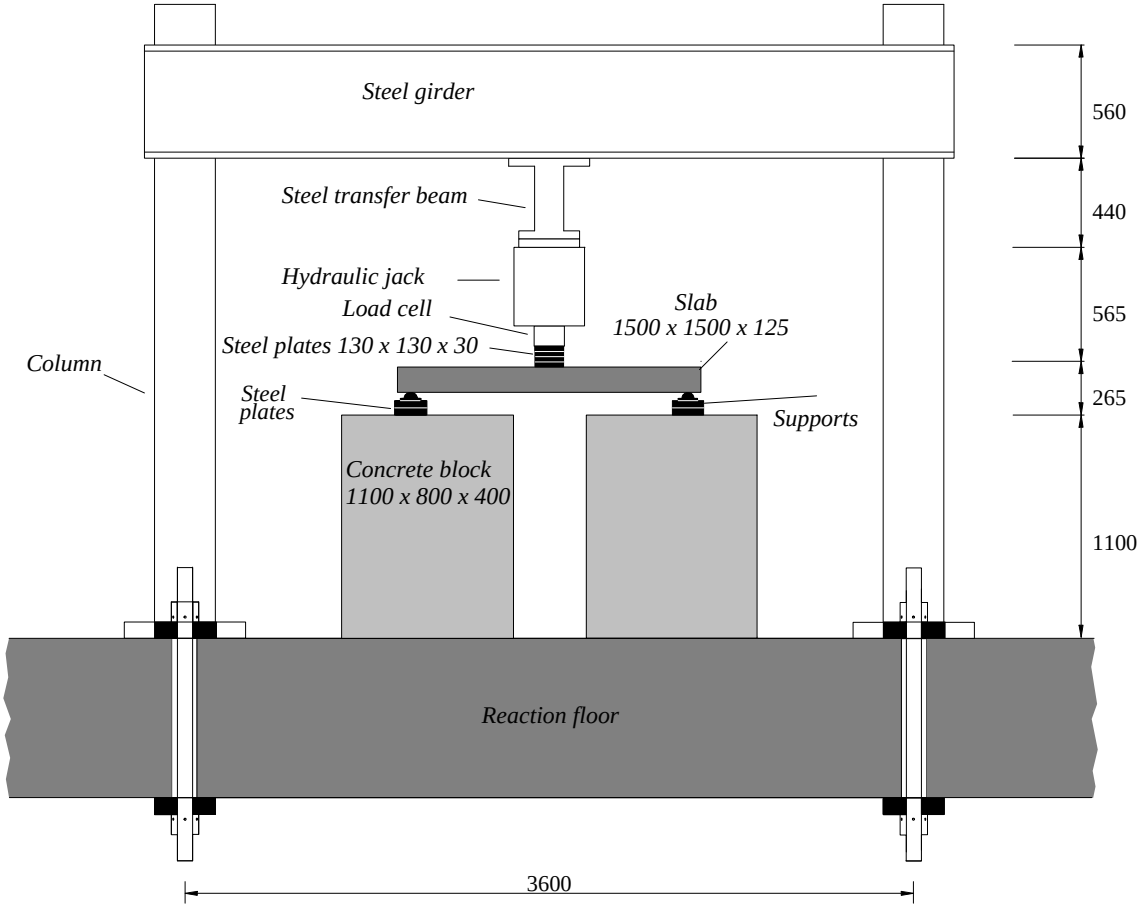

Figure 3.1: Test setup [mm]

The slab was simply supported on eight metallic supports in a circular pattern along the edge of the slab at the distance of 60 mm from the edge. The metallic supports were placed on four concrete blocks with the dimension of 1100 x 800 x 400 mm and the distance between consecutive supports was 575 mm. The slabs were free to undergo very large deformations after the punching failure, consequently, to allow the slabs to rotate and move without restraints, aluminum and teflon plates were placed between the support steel plates. Fig. 3.2 shows the locations and arrangement of the supports.

The concentrated load was applied on the center of the slab through a stack of three square steel plates with the dimension of 130 x 130 x 30 mm. The load was applied by the hydraulic jack with the maximum capacity of 2000 kN. The test was displacement controlled and the value of the applied force was measured by the load cell at defined time intervals. A 2 to 5 mm thick layer of plaster was placed between the slab and the steel plates to regularize the load introduction surfaces.

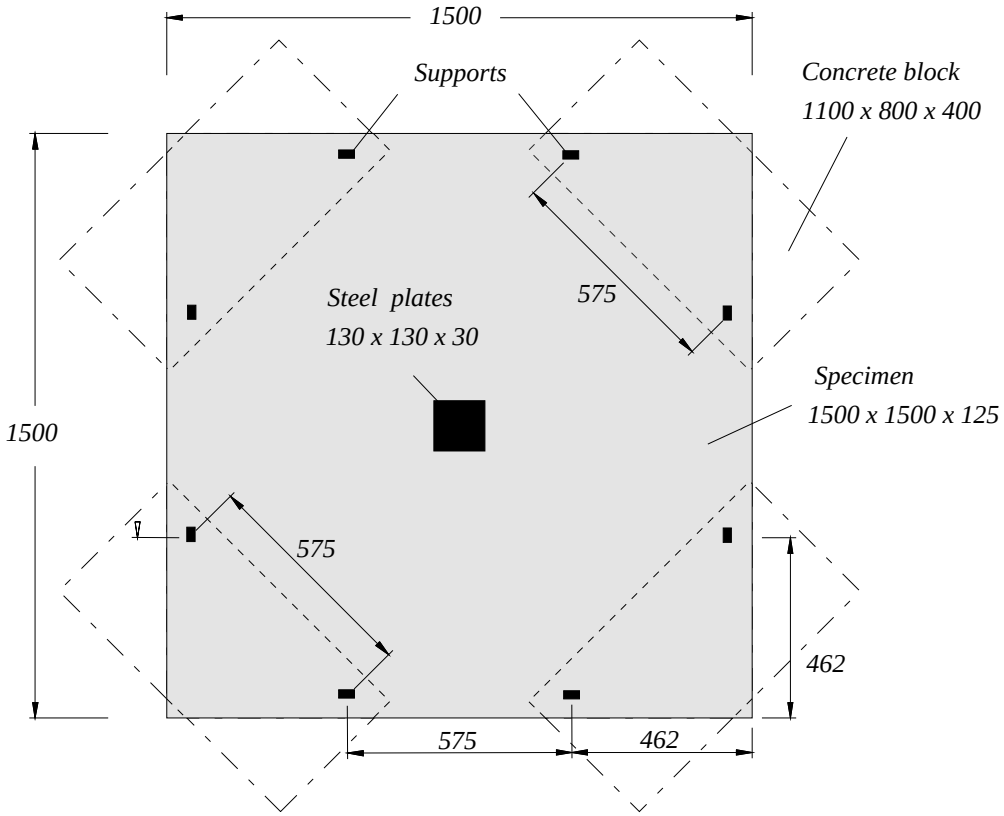

Figure 3.2 Test setup, plan view [mm]

3.2 Measurement instrumentation

Three different kind of measurement devices were used in these experiments. The force was measured using the load cell, the deflections were measured using LVDTs (linear variable displacement transducer), the variation of the thickness of the slab was measured using LVDTs, and the rotation of the slabs was measured using inclinometers. The time interval of the inclinometers measurements was about 10 seconds and for the other devices it was between 2 to 4 seconds. Fig. 3.3 shows the instrument setup at the bottom of a typical slab with the dimension of 1500 x 1500 x 125 mm. V1 measured the central displacement of the slab. Furthermore, V2 to V4 measured the deflection of the truncated punching cone symmetrically. In series 3, the number of LVDTs was increased to record the evolution of the slab displacement from support to the center of the slab, as shown in Fig. 3.3b. For the first and second test series, V2 to V5 were placed at a distance of 250 mm from the center of the slab. For the third series V2 to V4 were at the same position as in the two first series, V5 was placed at the distance of 125 mm from the center of the slab, and the additional transducers, V10 to V13, were placed in one single line with the distance of 125 mm from each other.

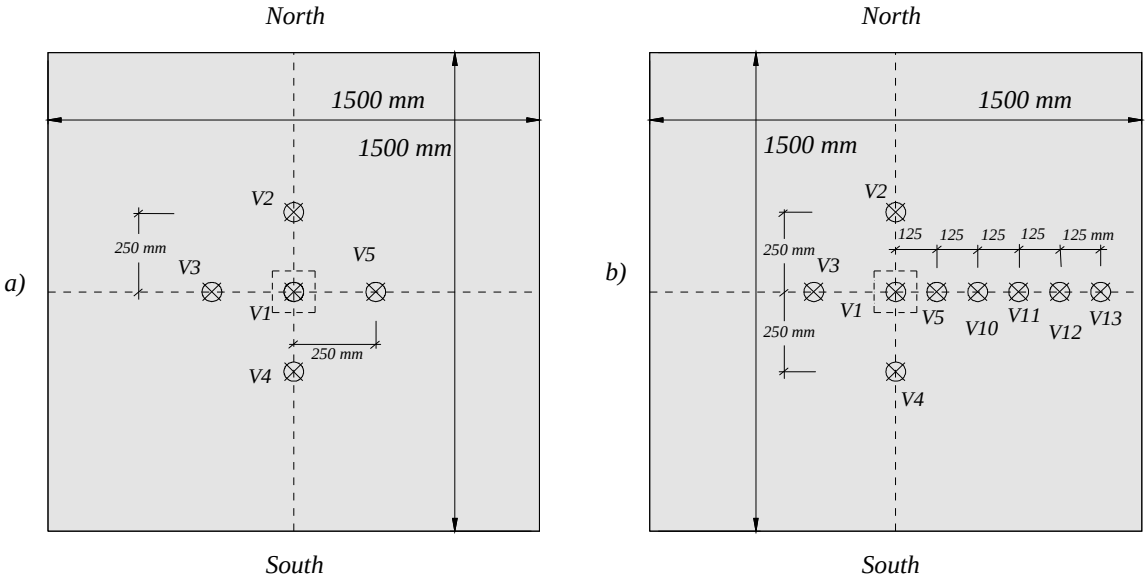

Figure 3.3: Instrument setup at the bottom of the slab for test series 1 and 2 (a), and for series 3 (b)

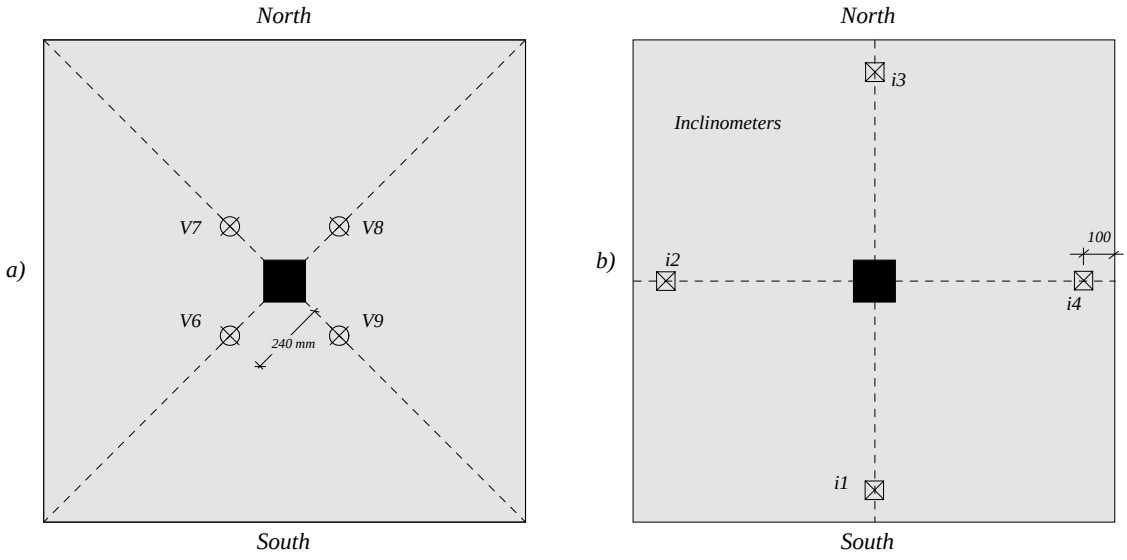

Figure 3.4: Instrument setup at the top of the slab for all test series

Fig. 3.4 shows the instrument layout at the top of the slab for all test series. V6 to V9 measured top surface displacement. V6 to V9 were placed at a distance of 240 mm from the center of the slab, whereas the inclinometers were placed at a distance of the 100 mm from the edge of the slab specimen.

One of the main objects of this experiment was to investigate the effect of the compressive reinforcement on the post-punching behavior of the concrete flat slabs supported by columns. The effect of compressive reinforcement is related to the relative displacement between the truncated punching cone and the rest of the slab. This relative penetration displacement was obtained as the difference between V14 and V15 as shown in Fig. 3.5.

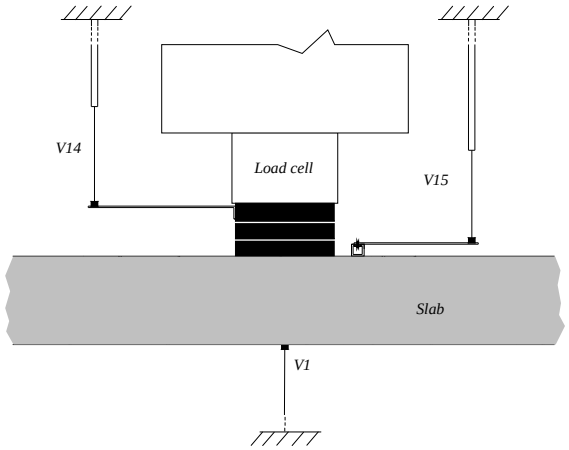

Figure 3.5: Instrument arrangement to measure the penetration displacement (V14 – V15)

Reinforcing bars play a great role in the post-punching behaviour of flat slabs supported by columns, because they are the only remaining link between the truncated punching cone and the rest of the slab. Thus the load carrying capacity of flat slabs after punching is significantly influenced by the amount and strength of reinforcingt steel. To gain a better understanding of the behaviour of the tensile reinforcement during and after punching failure, strain gauges were used to measure the elongation of the steel bars of the slabs PM-1 to PM-4. Fig. 3.6 shows the position of the strain gages.

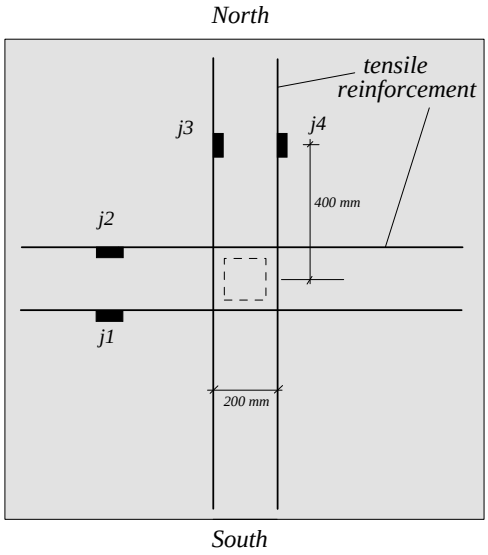

Figure 3.6: Layout of the strain gauges on the tensile reinforcement

4 Experimental results

Table 4.1 summarizes the main experimental results of this experimental campaign. The most important parameters are:

- V_p: Maximum load at punching failure
- w_p: Deflection corresponding to V_p
- V_{pp}: Maximum post-punching strength
- w_{pp}: Deflection corresponding to V_{pp}

Table 4.1: Summary of results for all the slabs

Test	ρ [%]	A_{sb}	V_p [kN]	w_p [mm]	V_{pp} [kN]	w_{pp} [mm]	$\frac{V_{pp}}{V_p}$
PM-1	0.25	-	175.8	13.6	37.2	70.5	0.21
PM-2	0.49	-	223.7	11.0	66.0	52.7	0.30
PM-3	0.82	-	324.3	13.1	117.4	45.3	0.36
PM-4	1.41	-	295.2	7.4	107.8	42.6	0.37
PM-9	0.82	4Ø8	224.2	7.1	123.4	36.2	0.55
PM-10	0.82	4Ø10	227.5	6.7	158.6	42.9	0.70
PM-11	0.82	4Ø12	240.6	8.2	236.5	86.3	0.98
PM-12	0.82	4Ø14	249.0	8.2	245.0	116.9	0.98
PM-13	0.82	4Ø8*	326.7	11.4	150.6	39.9	0.46
PM-14	0.82	4Ø10*	355.8	12.6	187.5	71.7	0.53
PM-15	0.84	4Ø12*	274.0	9.1	176.7	66.5	0.64
PM-16	0.83	4Ø14*	298.4	10.1	134.8	43.4	0.45
PM-17	0.82	4Ø8**	329.1	15.1	246.6	50.0	0.75
PM-18	0.88	4Ø10**	322.7	15.7	236.7	56.5	0.73
PM-19	0.85	4Ø12**	417.3	28.7	315.0	90.1	0.75
PM-20	0.82	4Ø14**	402.1	19.3	344.9	95.2	0.86
PM-21	0.81	4Ø8	255.7	9.7	185.4	42.9	0.73
PM-22	0.85	4Ø10	288.2	14.1	218.7	65.2	0.76
PM-23	0.88	-	227.0	10.4	82.2	83.0	0.36
PM-24	0.86	-	271.5	12.1	100.6	74.2	0.37
PM-25	0.85	4Ø8	143.0	7.7	85.4+	69.8	0.60
PM-26	0.83	4Ø10	164.7	8.5	104.6+	89.3	0.64
PM-27	0.81	4Ø12	211.2	8.0	94.1+	64.1	0.45
PM-28	0.85	4Ø14	257.6	11.2	101.4+	57.2	0.39

* Bent-up bars with insufficient anchorage length

** Well-anchored bent-up bars

+ Test was terminated due to the risk of falling down the punching cone

In this chapter the experimental results are shown for each slab specimen including the following parts:

- Graph (a): Load versus central slab deflection (V1).
- Graph (b): Load versus rotation of the slab, measured with the inclinometers, i1, i2, i3 and i4. This curve is shown up to the initial punching failure due to the fact that the experimental results obtained beyond this point were rather random: N – S: average of i1 and i3, E – O: average of i2 and i4.
- Graph (c): Load versus relative penetration displacement δ between the truncated punching cone and the rest of the slab specimen. This relative displacement was measured using V14 and V15.
- Graph (d): Load versus average deflection of the compression side of the slab at the distance of 240 mm from the center, expressed as the average of V6, V7, V8 and V9. This curve is truncated after the initial punching shear failure as for graph (b).
- Graph (e): For PM-1 to PM-16 is slab plan view after testing. For PM-17 to PM-28 is slab section after testing accompanied by the evolution of the slab deflection at representative load levels.

$\rho = 0.25\%$ $f_c = 36.6\ MPa$

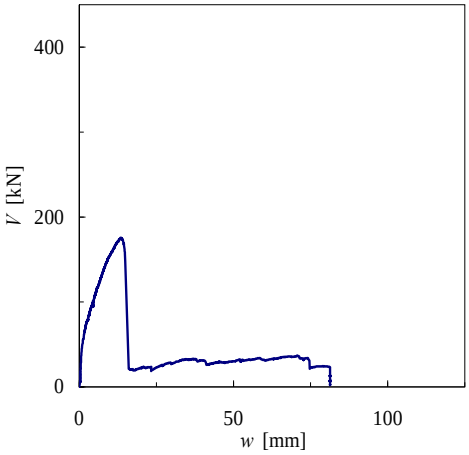

(a) *Load - central deflection*

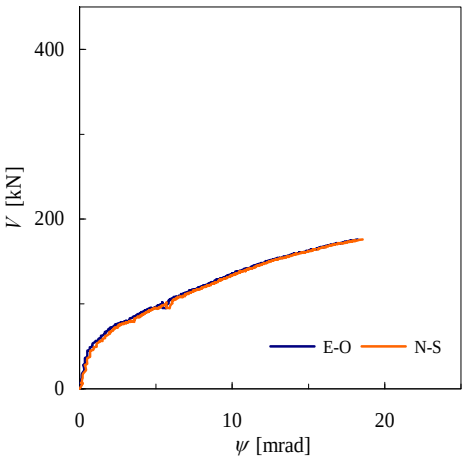

(b) *Load - rotation up to punching*

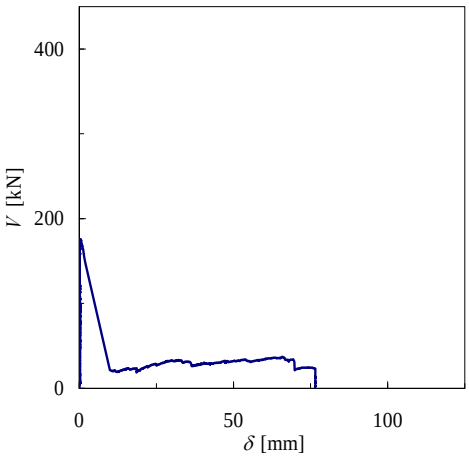

(c) *Load - penetration displacement*

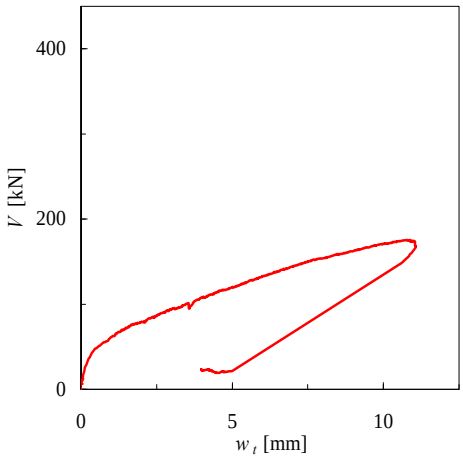

(d) *Load - compression side deflection*

(e) *Slab plan view after testing*

Figure 4.1: Slab PM-1: membrane effect, ρ = 0.25%

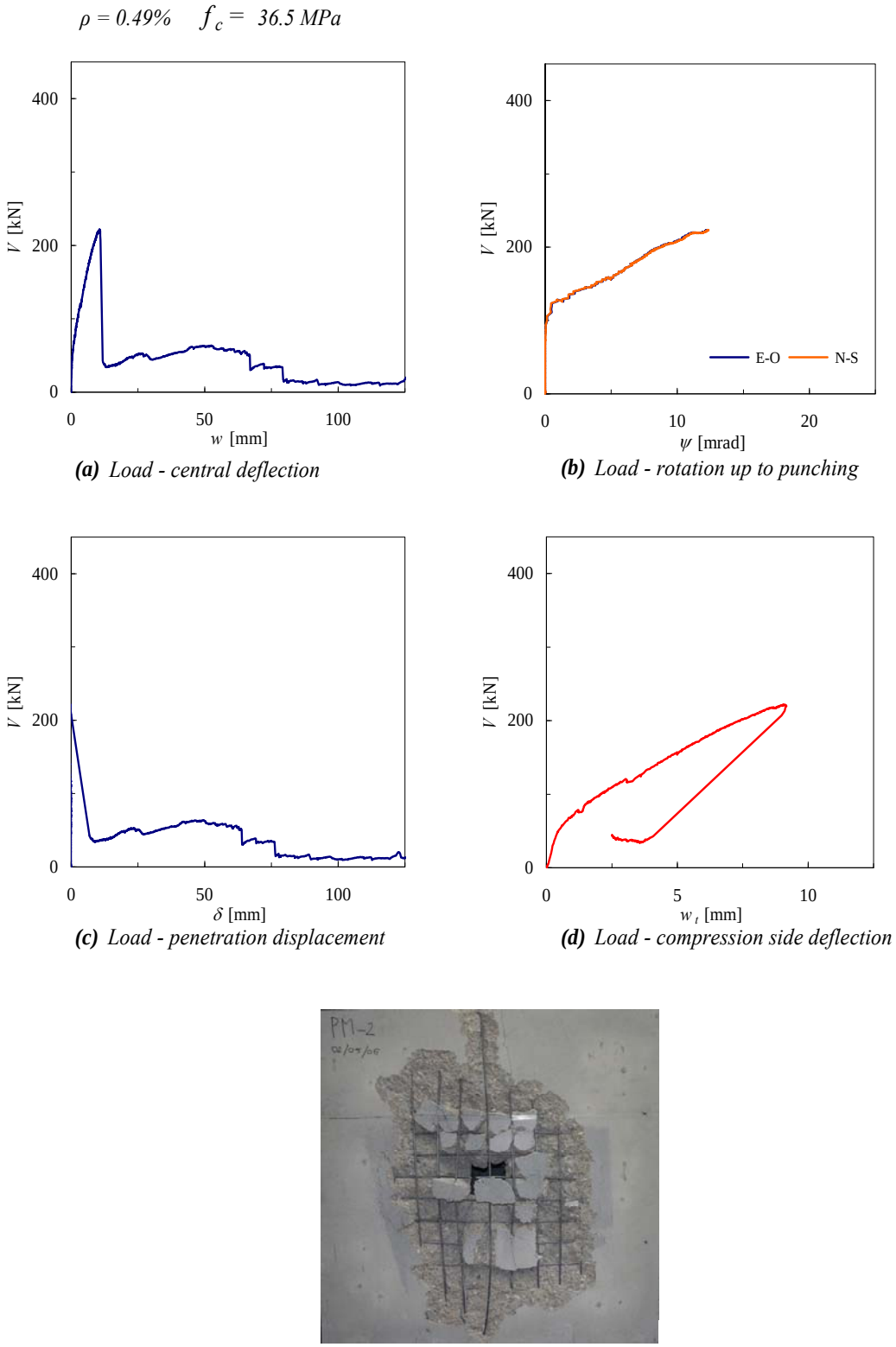

(a) *Load - central deflection*

(b) *Load - rotation up to punching*

(c) *Load - penetration displacement*

(d) *Load - compression side deflection*

(e) *Slab plan view after testing*

Figure 4.2: Slab PM-2: membrane effect, ρ = 0.49%

$\rho = 0.82\%$ $f_c = 37.8\ MPa$

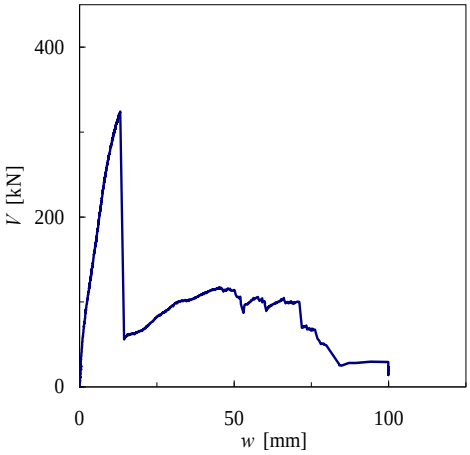

(a) *Load - central deflection*

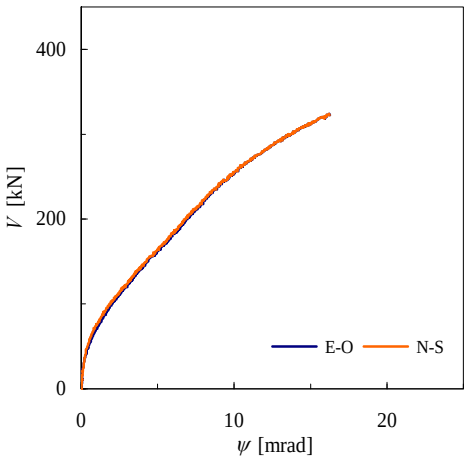

(b) *Load - rotation up to punching*

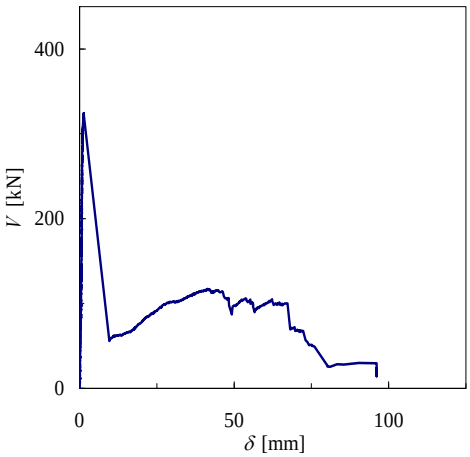

(c) *Load - penetration displacement*

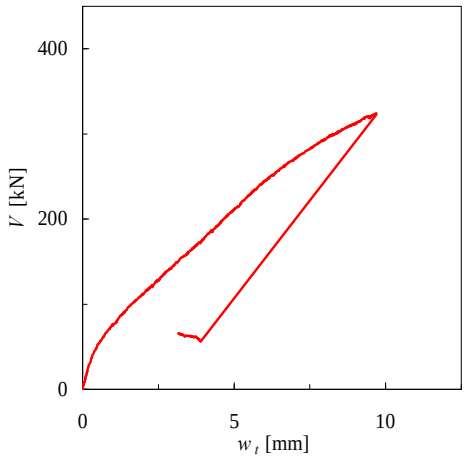

(d) *Load - compression side deflection*

(e) *Slab plan view after testing*

Figure 4.3: Slab PM-3: membrane effect, ρ = 0.82%

$\rho = 1.41\%$ $f_c = 36.8$ MPa

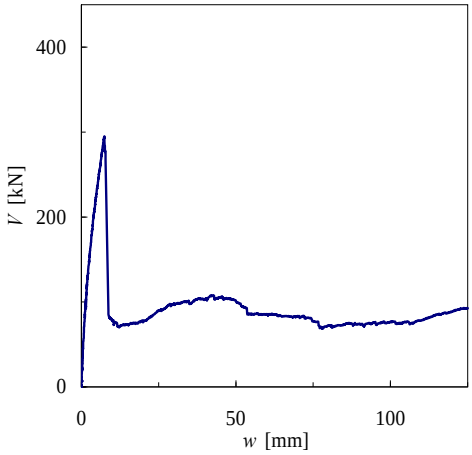

(a) *Load - central deflection*

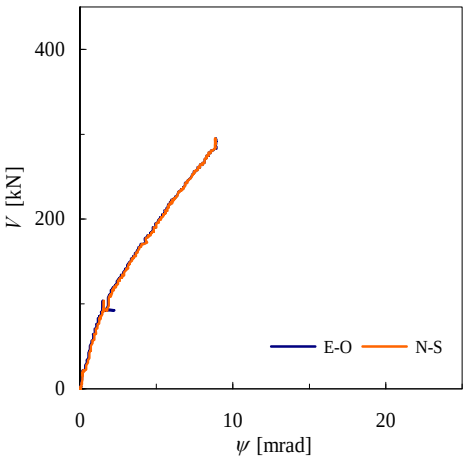

(b) *Load - rotation up to punching*

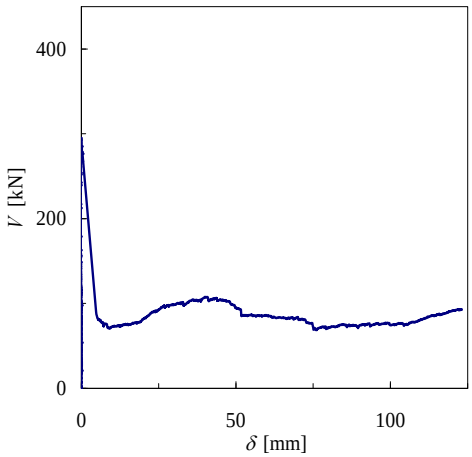

(c) *Load - penetration displacement*

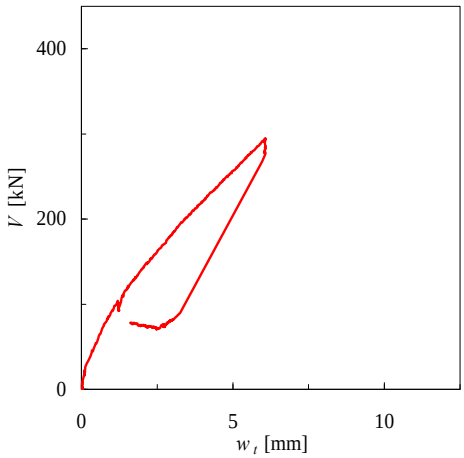

(d) *Load - compression side deflection*

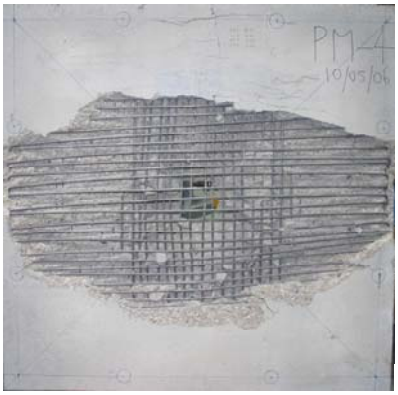

(e) *Slab plan view after testing*

Figure 4.4: Slab PM-4: membrane effect, ρ = 1.41%

$\rho = 0.82\%$ $f_c = 31$ MPa

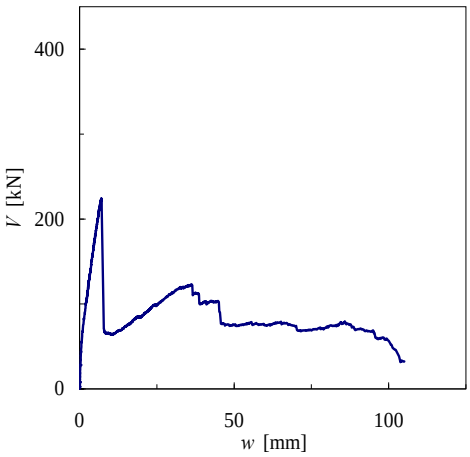

(a) *Load - central deflection*

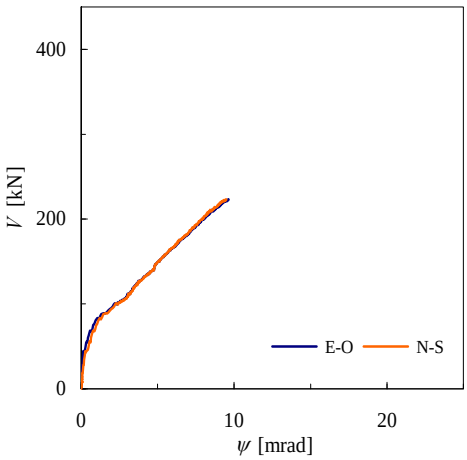

(b) *Load - rotation up to punching*

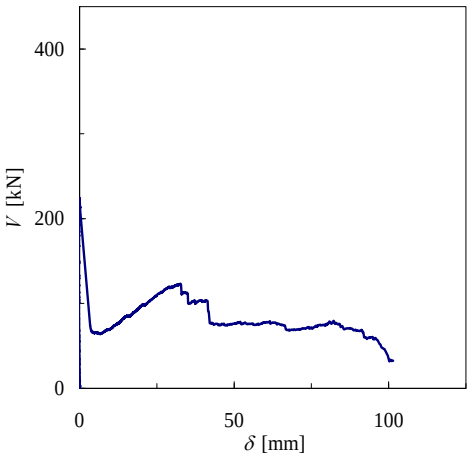

(c) *Load - penetration displacement*

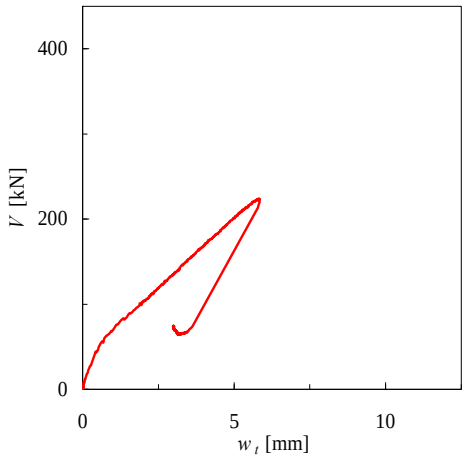

(d) *Load - compression side deflection*

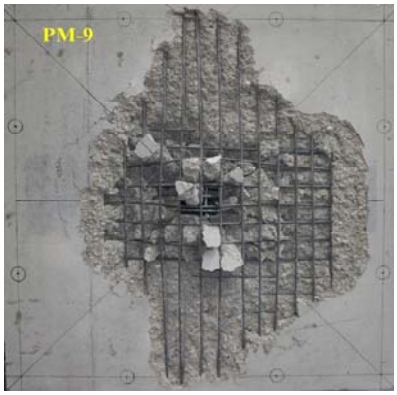

(e) *Slab plan view after testing*

Figure 4.5: Slab PM-9: straight compressive bars for dowel action Ø8

$\rho = 0.82\%$ $f_c = 31.1$ MPa

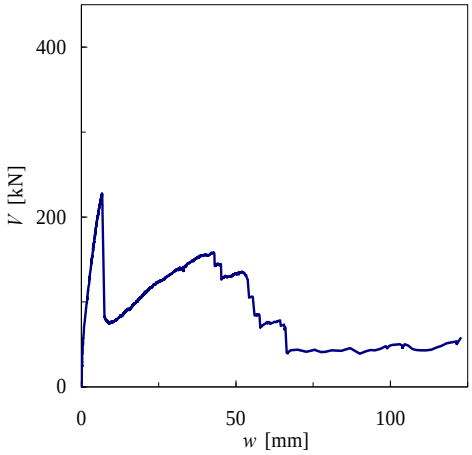

(a) *Load - central deflection*

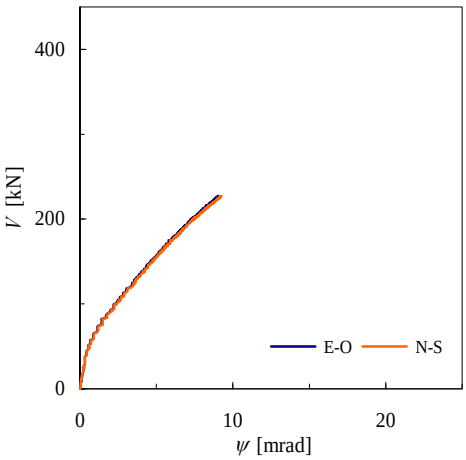

(b) *Load - rotation up to punching*

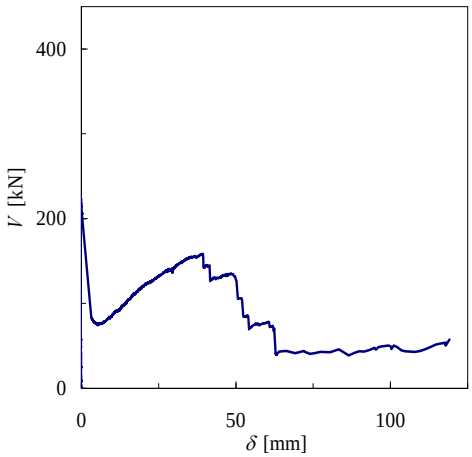

(c) *Load - penetration displacement*

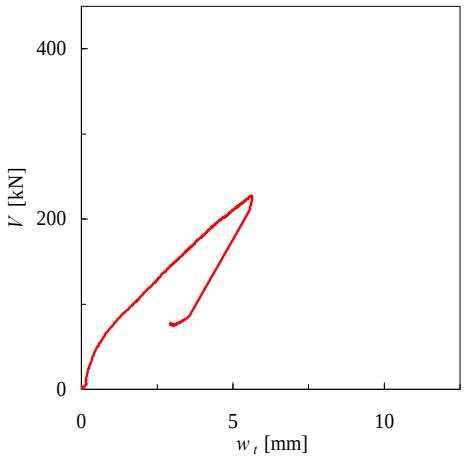

(d) *Load - compression side deflection*

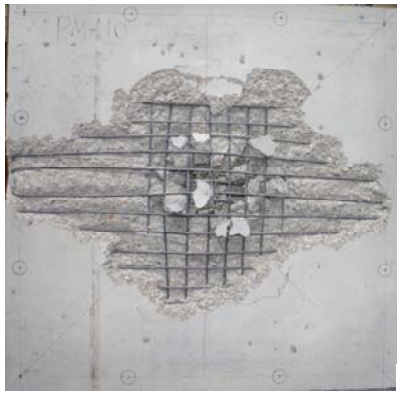

(e) Slab plan view after testing

Figure 4.6: Slab PM-10: straight compressive bars for dowel action Ø10

$\rho = 0.82\%$ $f_c = 32.3\ MPa$

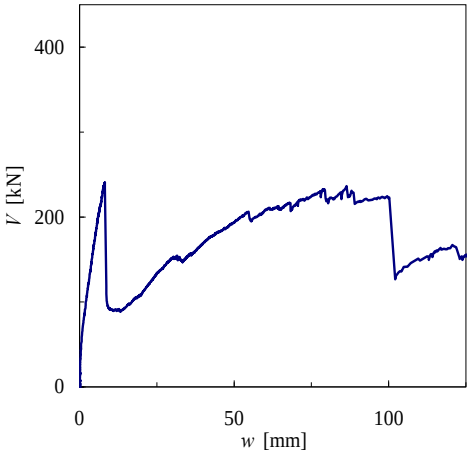

(a) *Load - central deflection*

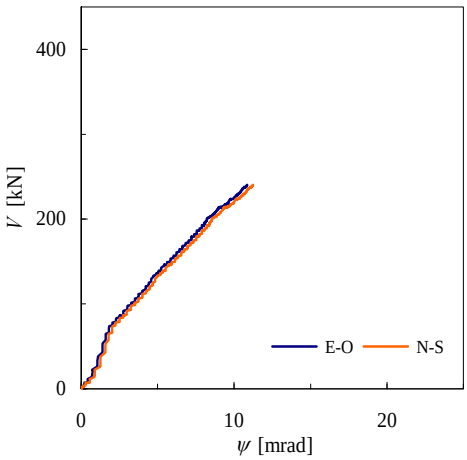

(b) *Load - rotation up to punching*

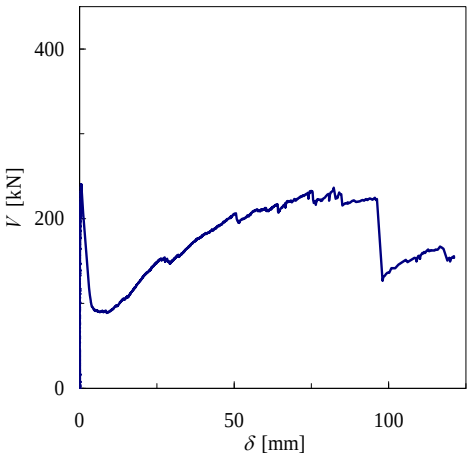

(c) *Load - penetration displacement*

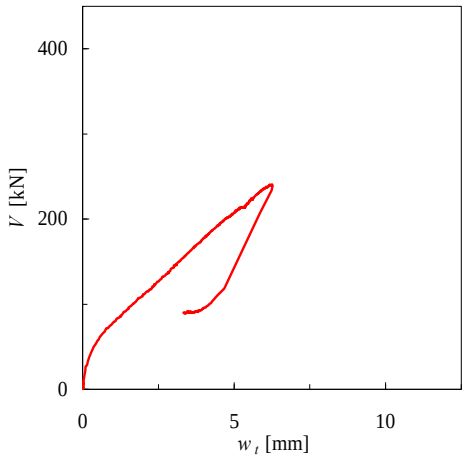

(d) *Load - compression side deflection*

(e) *Slab plan view after testing*

Figure 4.7: Slab PM-11: straight compressive bars for dowel action Ø12

$\rho = 0.82\%$ $f_c = 32.4$ MPa

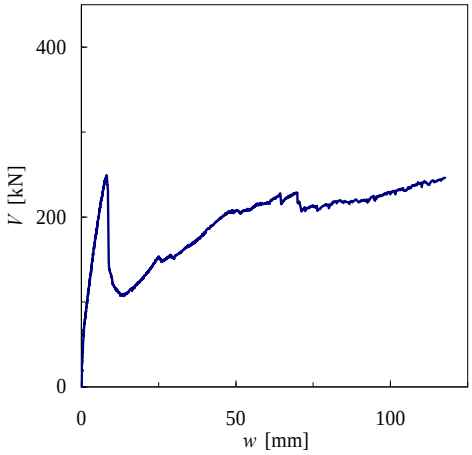

(a) *Load - central deflection*

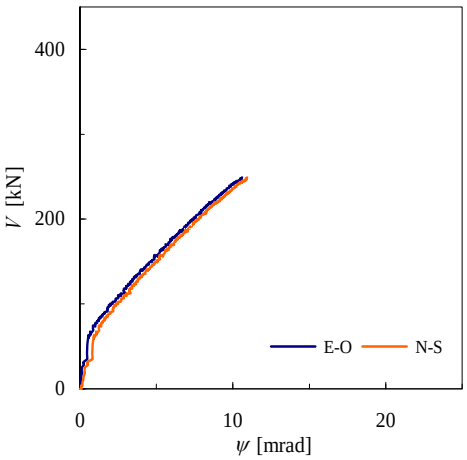

(b) *Load - rotation up to punching*

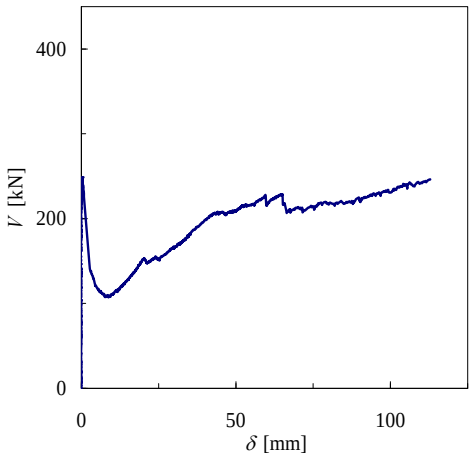

(c) *Load - penetration displacement*

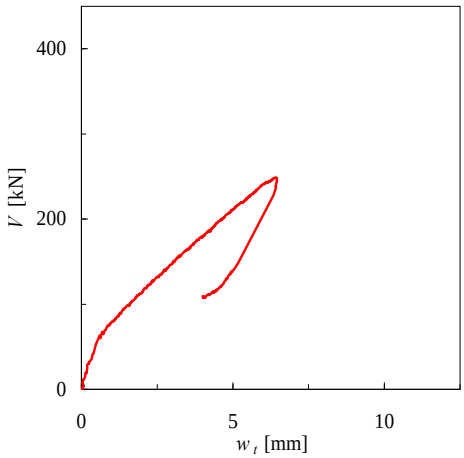

(d) *Load - compression side deflection*

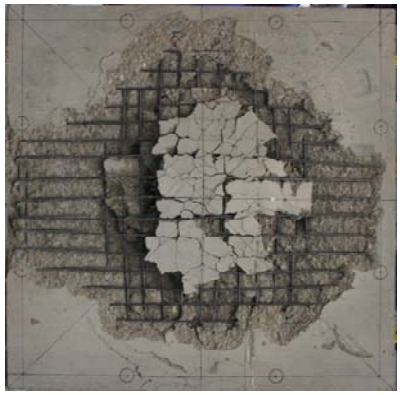

(e) Slab plan view after testing

Figure 4.8: Slab PM-12: straight compressive bars for dowel action Ø14

$\rho = 0.82\%$ $f_c = 32.6\ MPa$

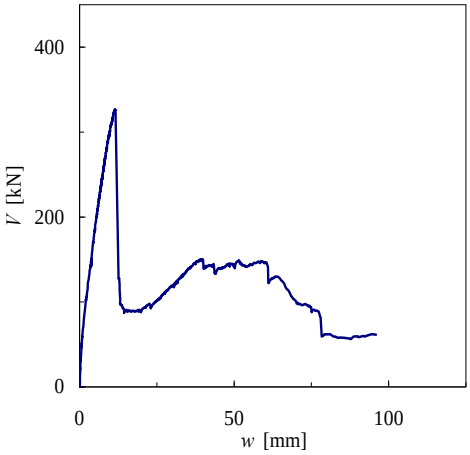

(a) *Load - central deflection*

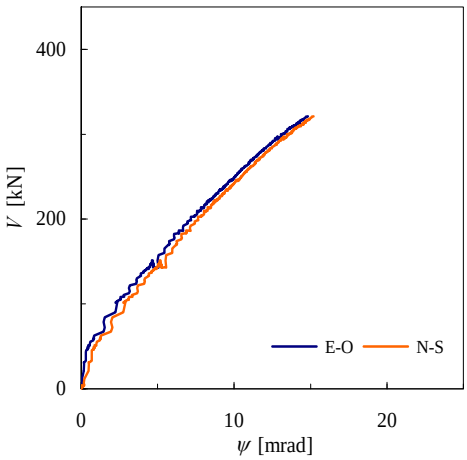

(b) *Load - rotation up to punching*

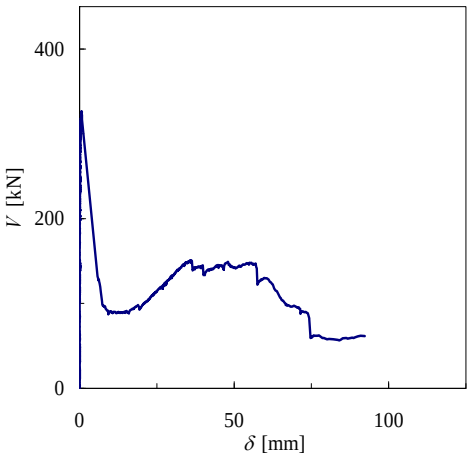

(c) *Load - penetration displacement*

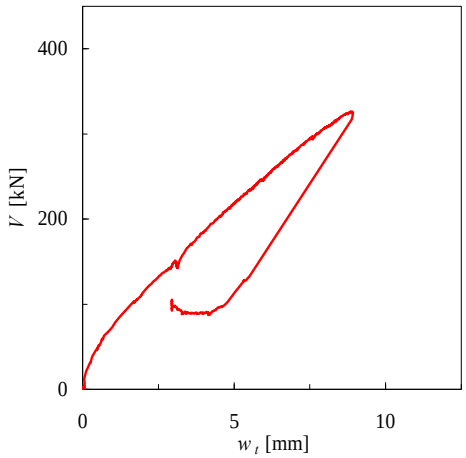

(d) *Load - compression side deflection*

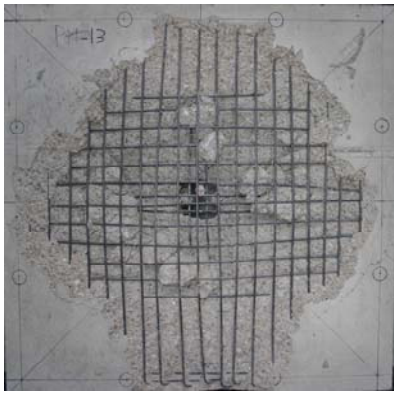

(e) *Slab plan view after testing*

Figure 4.9: Slab PM-13: bent-up-bars Ø8, insufficient anchorage

$\rho = 0.82\%$ $f_c = 32.7\ MPa$

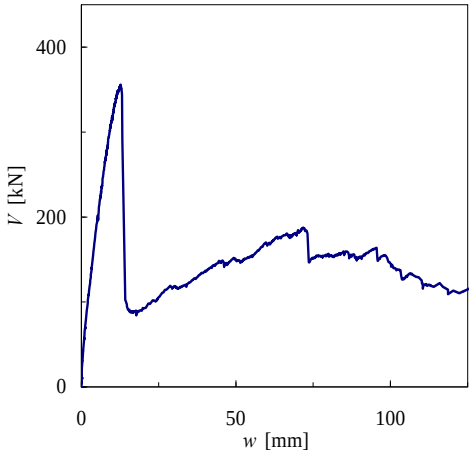

(a) *Load - central deflection*

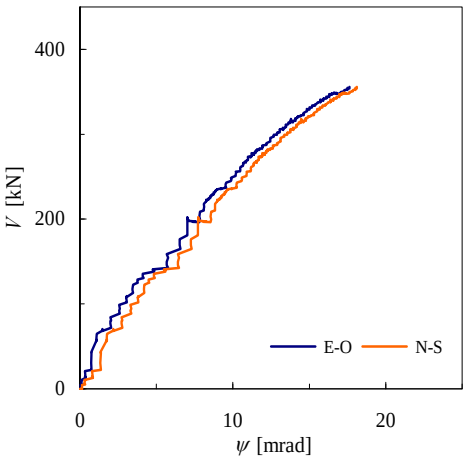

(b) *Load - rotation up to punching*

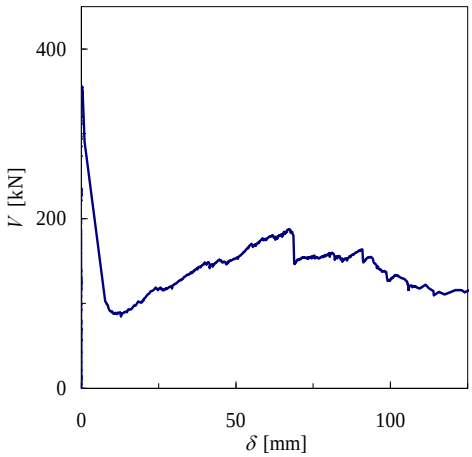

(c) *Load - penetration displacement*

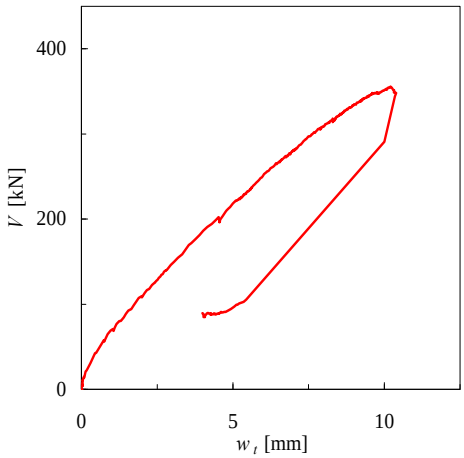

(d) *Load - compression side deflection*

(e) *Slab plan view after testing*

Figure 4.10: Slab PM-14: bent-up-bars Ø10, insufficient anchorage

$\rho = 0.84\%$ $f_c = 32.7\ MPa$

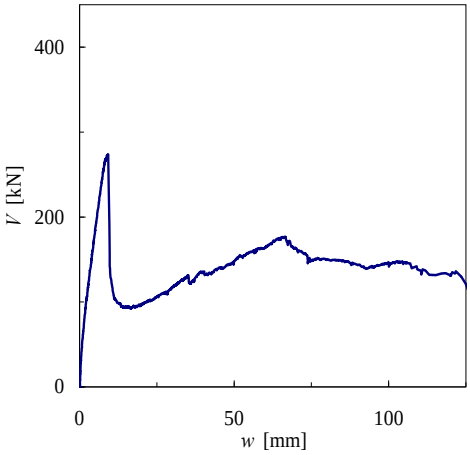

(a) *Load - central deflection*

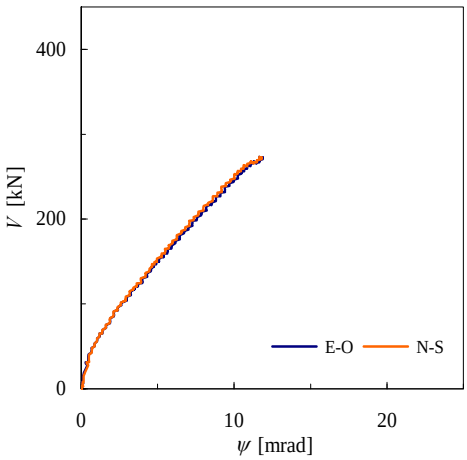

(b) *Load - rotation up to punching*

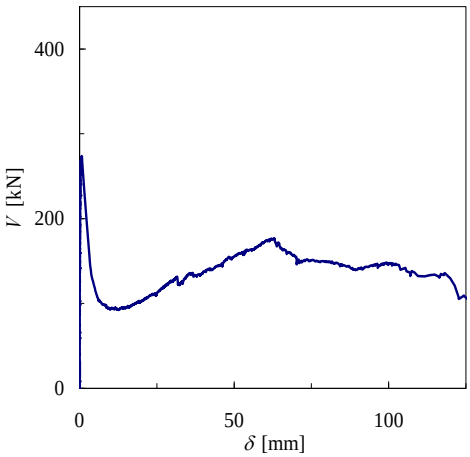

(c) *Load - penetration displacement*

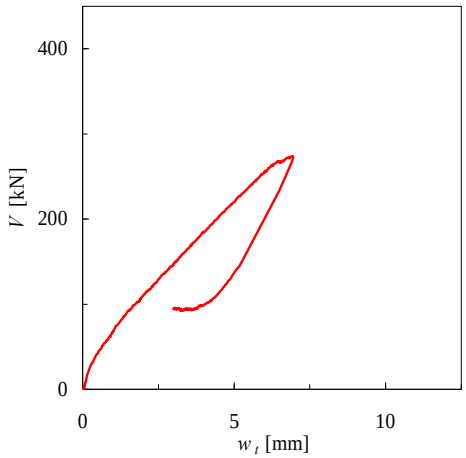

(d) *Load - compression side deflection*

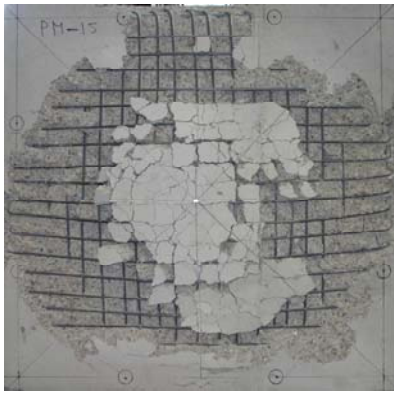

(e) *Slab plan view after testing*

Figure 4.11: Slab PM-15: bent-up-bars Ø12, insufficient anchorage

$\rho = 0.83\%$ $f_c = 32.8$ MPa

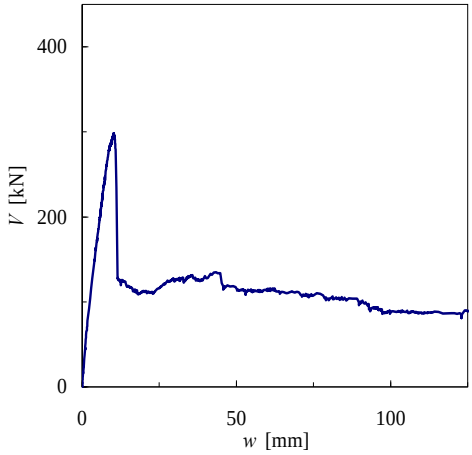

(a) *Load - central deflection*

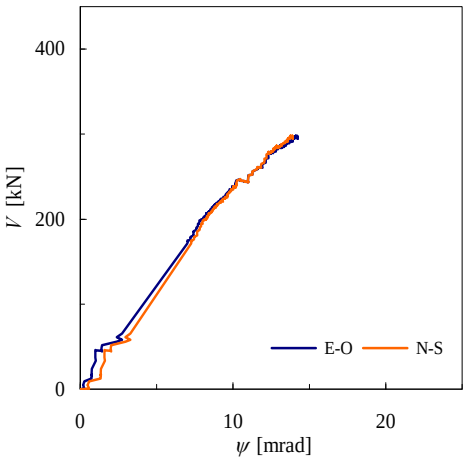

(b) *Load - rotation up to punching*

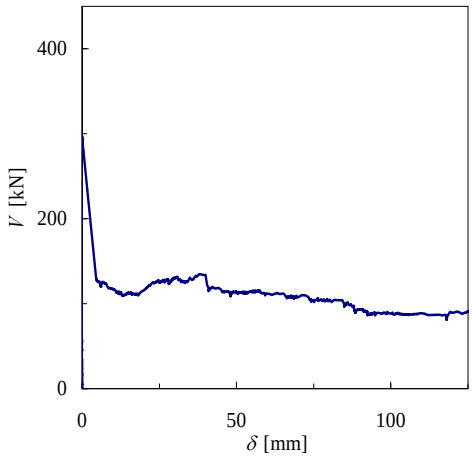

(c) *Load - penetration displacement*

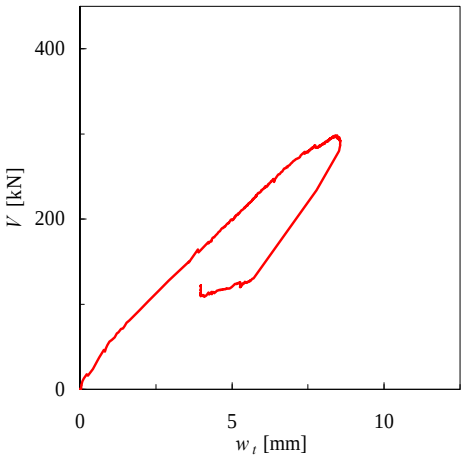

(d) *Load - compression side deflection*

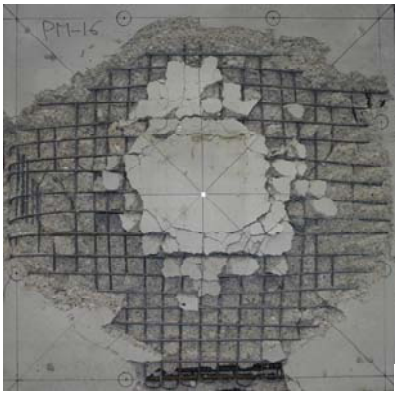

(e) *Slab plan view after testing*

Figure 4.12: Slab PM-16: bent-up-bars Ø14, insufficient anchorage

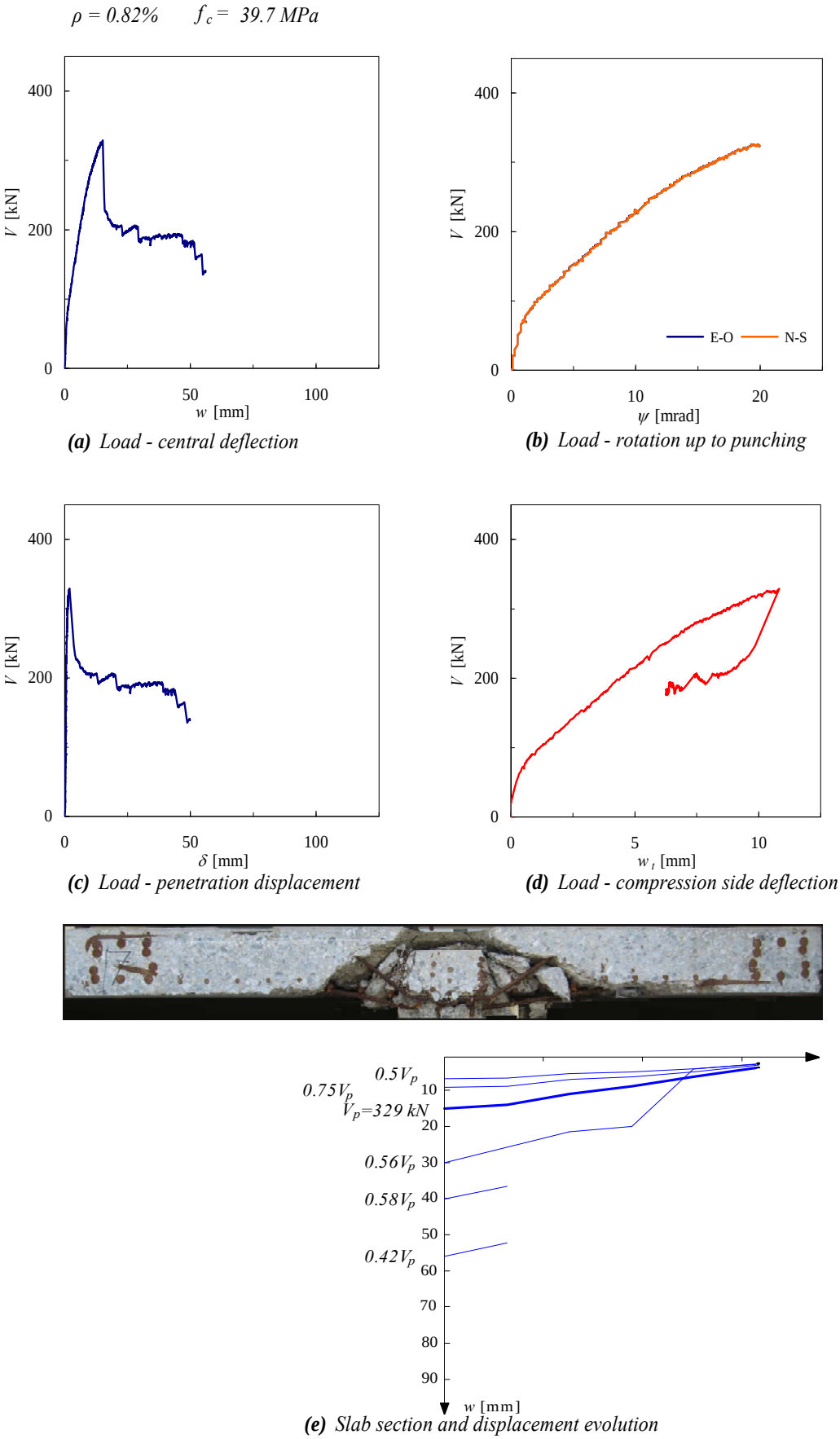

(a) *Load - central deflection*

(b) *Load - rotation up to punching*

(c) *Load - penetration displacement*

(d) *Load - compression side deflection*

(e) *Slab section and displacement evolution*

Figure 4.13: Slab PM-17: fully anchored bent-up-bars Ø8

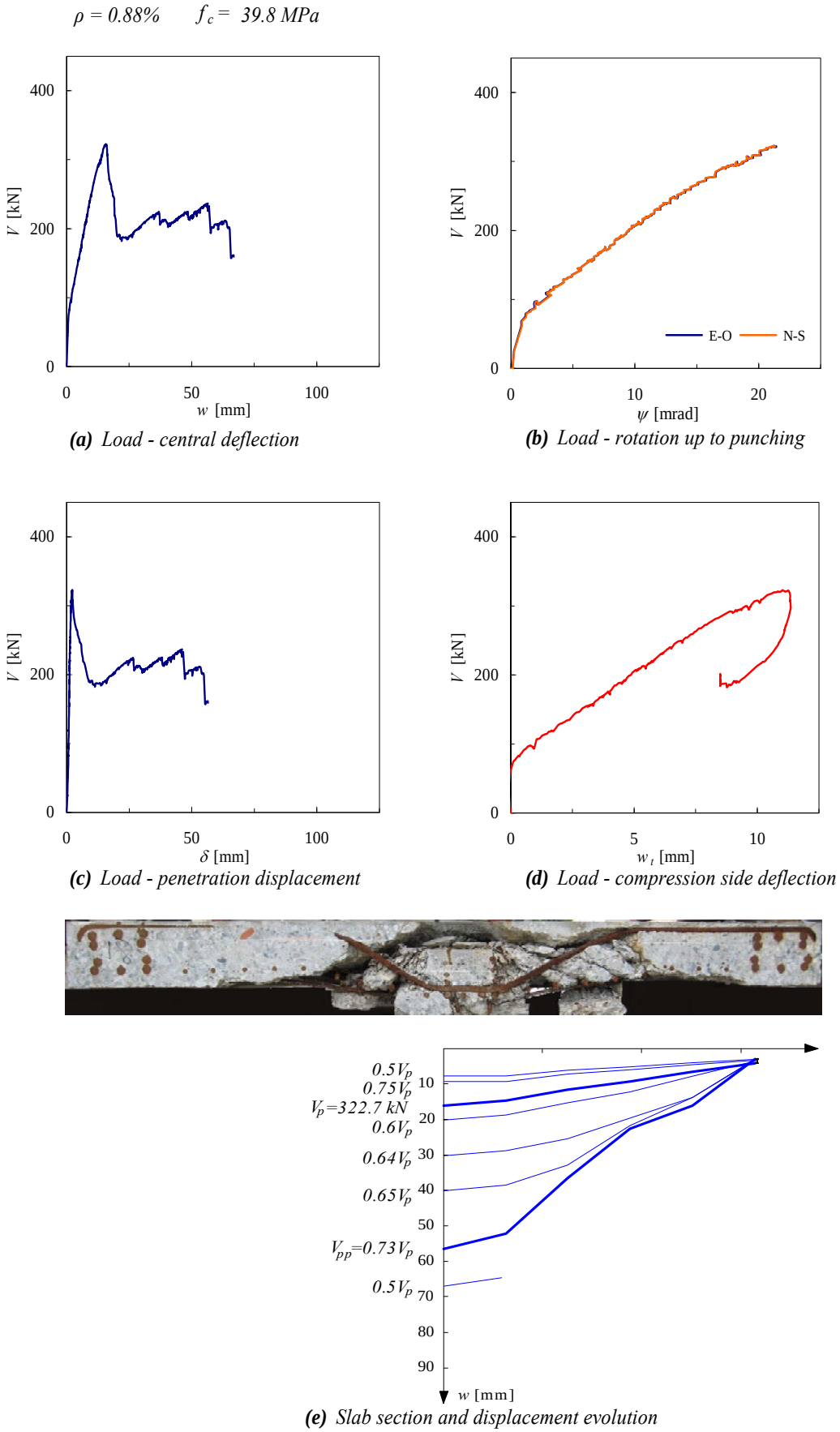

(a) *Load - central deflection*

(b) *Load - rotation up to punching*

(c) *Load - penetration displacement*

(d) *Load - compression side deflection*

(e) *Slab section and displacement evolution*

Figure 4.14: Slab PM-18: fully anchored bent-up-bars Ø10

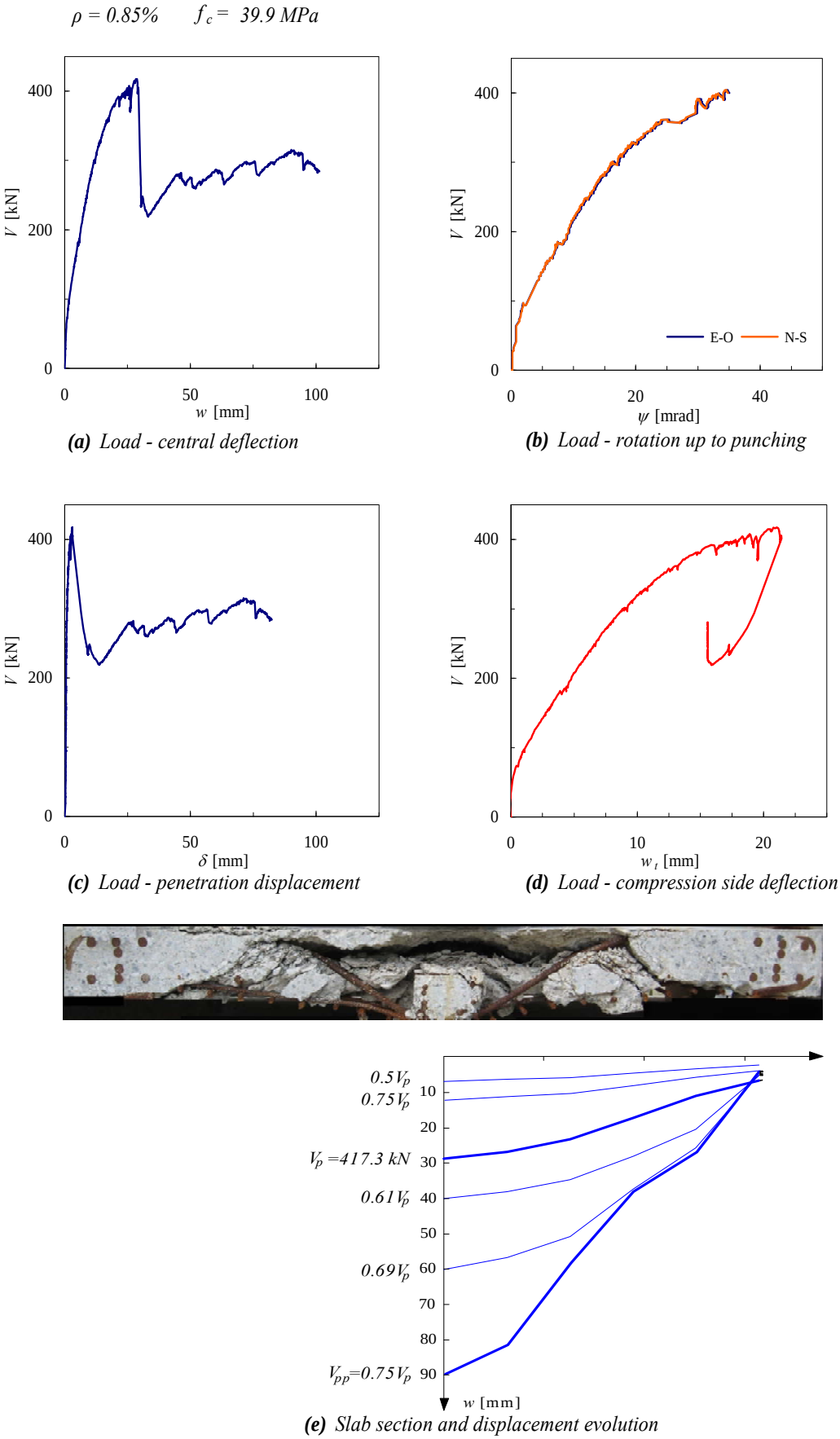

(a) *Load - central deflection*

(b) *Load - rotation up to punching*

(c) *Load - penetration displacement*

(d) *Load - compression side deflection*

(e) *Slab section and displacement evolution*

Figure 4.15: Slab PM-19: fully anchored bent-up-bars Ø12

$\rho = 0.82\%$ $f_c = 40\ MPa$

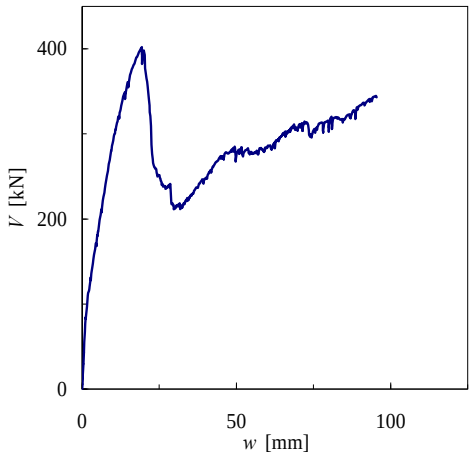

(a) *Load - central deflection*

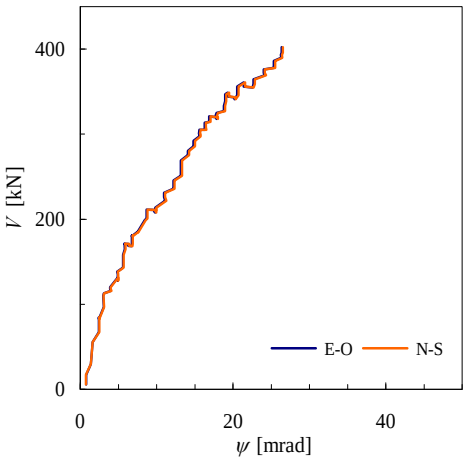

(b) *Load - rotation up to punching*

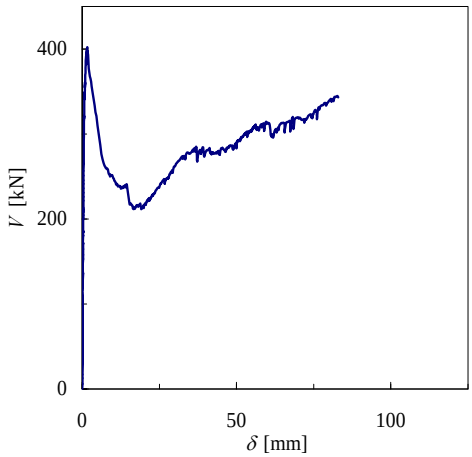

(c) *Load - penetration displacement*

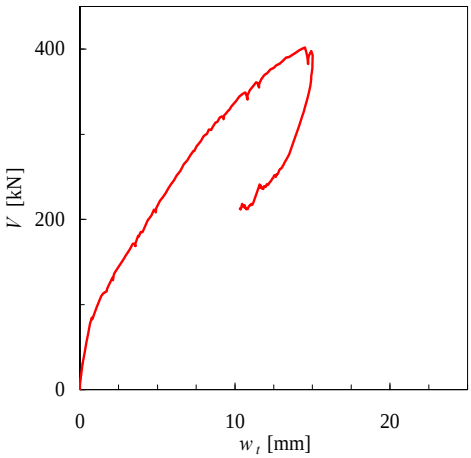

(d) *Load - compression side deflection*

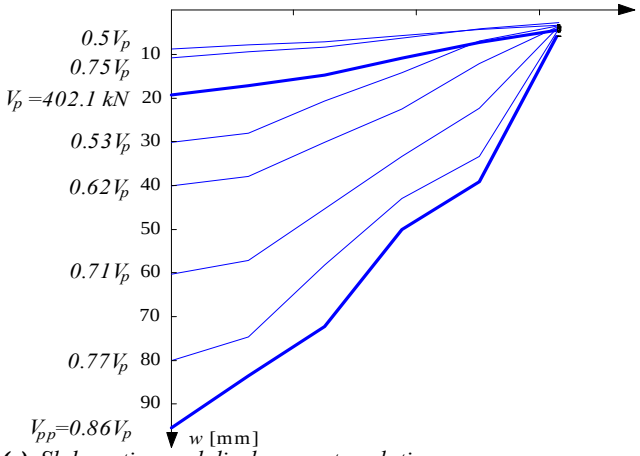

(e) *Slab section and displacement evolution*

Figure 4.16: Slab PM-20: fully anchored bent-up-bars Ø14

$\rho = 0.81\%$ $f_c = 40.2$ MPa

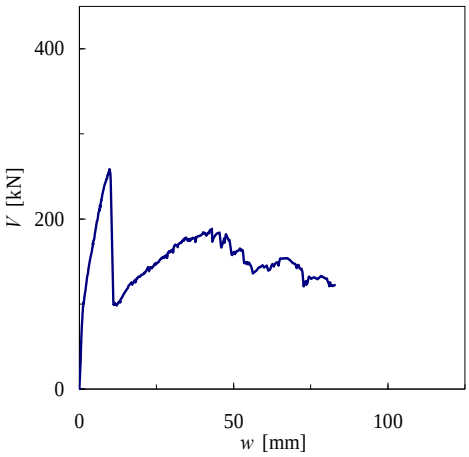

(a) *Load - central deflection*

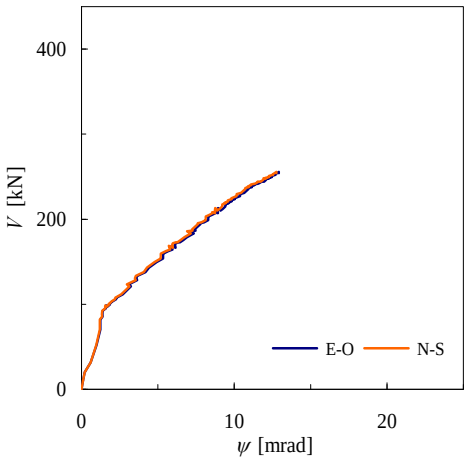

(b) *Load - rotation up to punching*

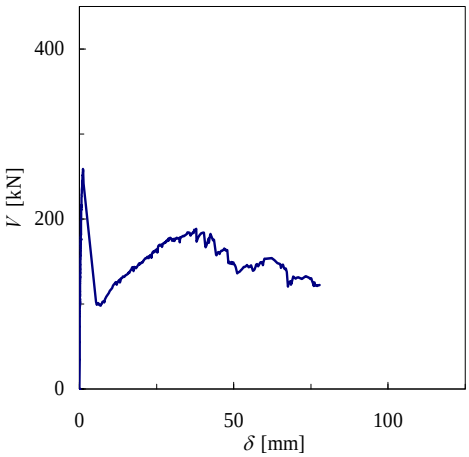

(c) *Load - penetration displacement*

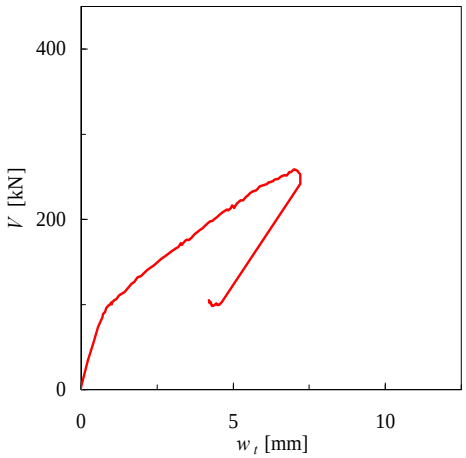

(d) *Load - compression side deflection*

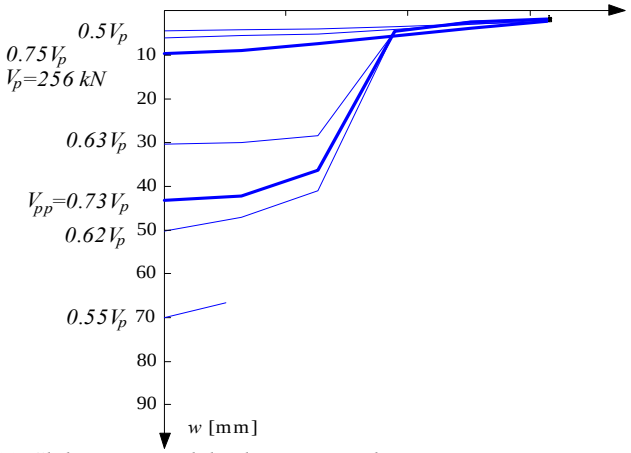

(e) *Slab section and displacement evolution*

Figure 4.17: Slab PM-21: straight compressive reinforcement Ø8

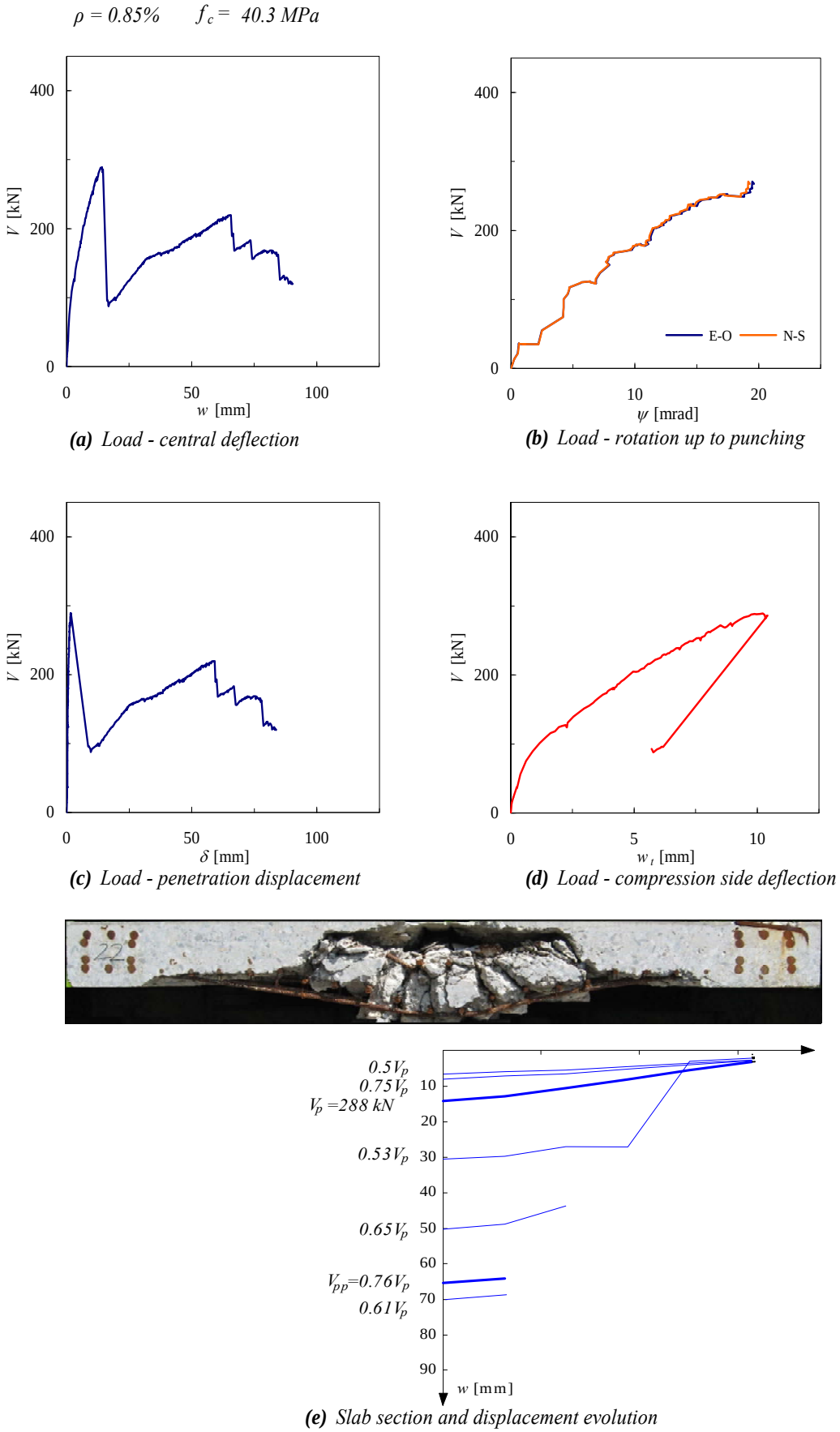

(a) *Load - central deflection*

(b) *Load - rotation up to punching*

(c) *Load - penetration displacement*

(d) *Load - compression side deflection*

(e) *Slab section and displacement evolution*

Figure 4.18: Slab PM-22: straight compressive reinforcement Ø10, hot-rolled steel

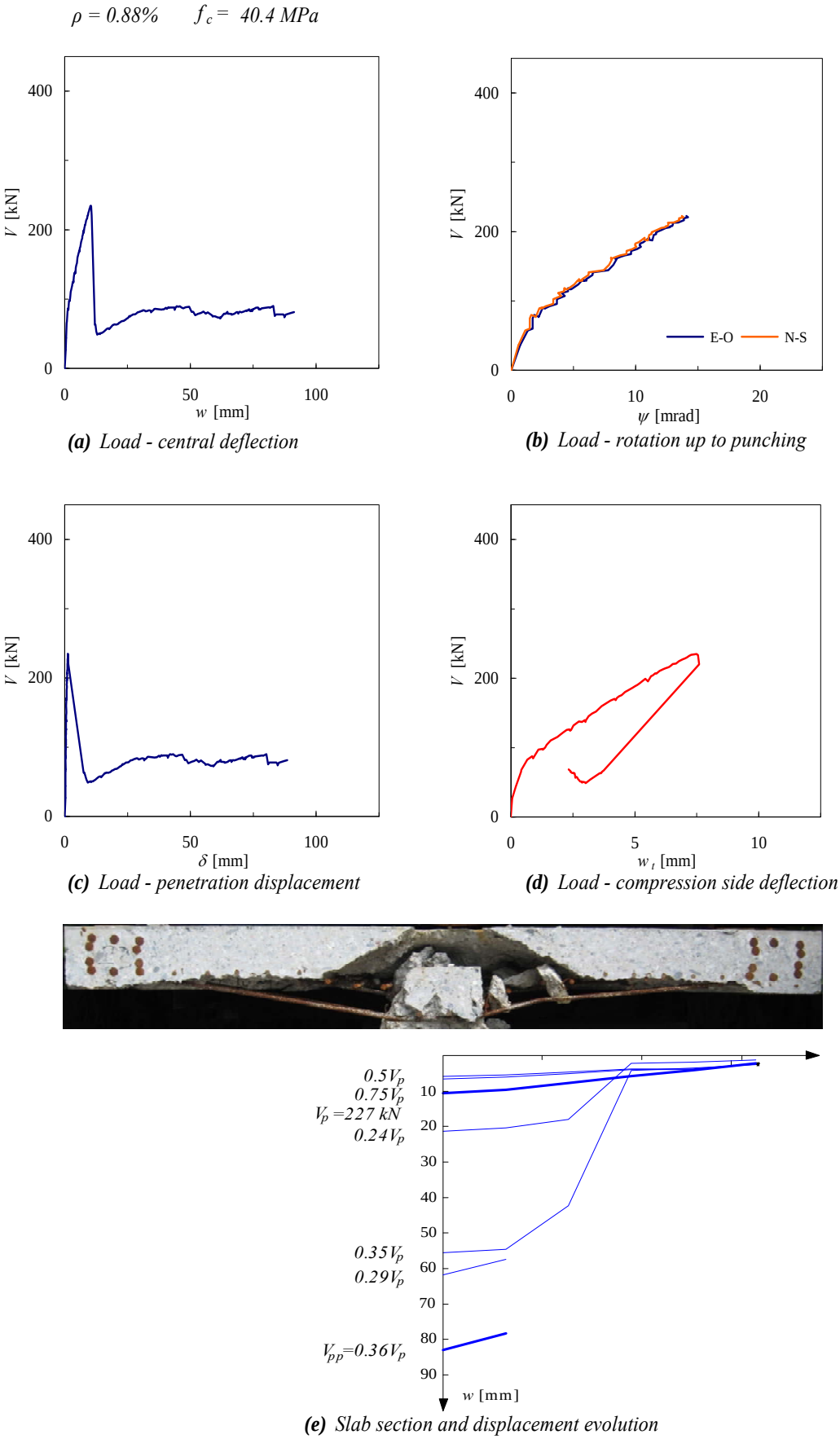

(a) *Load - central deflection*

(b) *Load - rotation up to punching*

(c) *Load - penetration displacement*

(d) *Load - compression side deflection*

(e) *Slab section and displacement evolution*

Figure 4.19: Slab PM-23: membrane effect, ρ = 0.88%

$\rho = 0.86\%$ $f_c = 40.4$ MPa

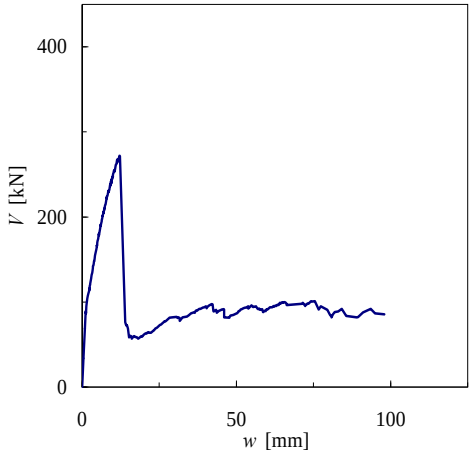

(a) *Load - central deflection*

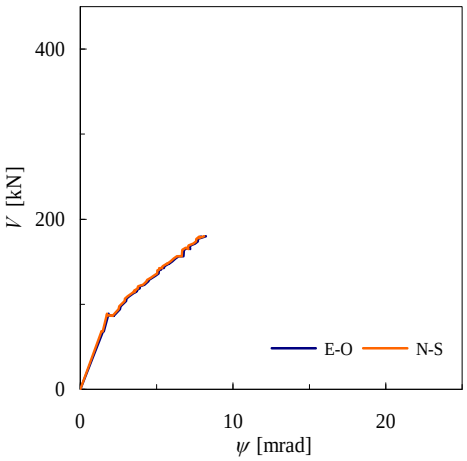

(b) *Load - rotation up to punching*

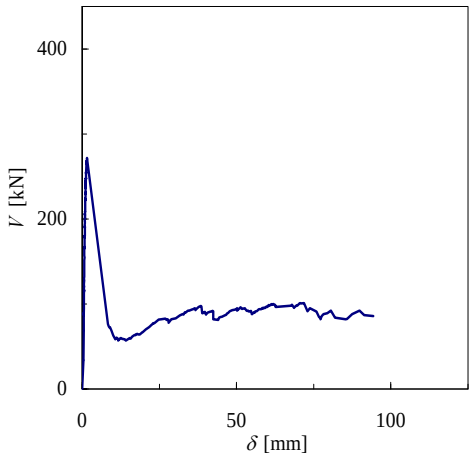

(c) *Load - penetration displacement*

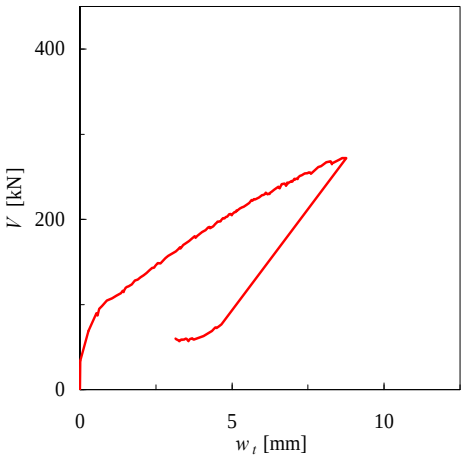

(d) *Load - compression side deflection*

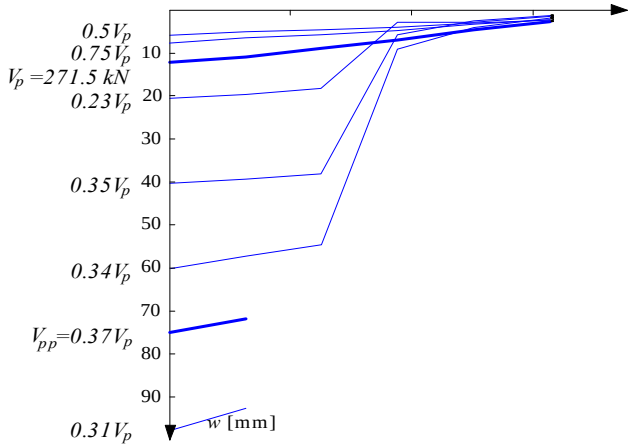

(e) *Slab section and displacement evolution*

Figure 4.20: Slab PM-24: membrane effect, ρ = 0.85%, confinement reinforcement

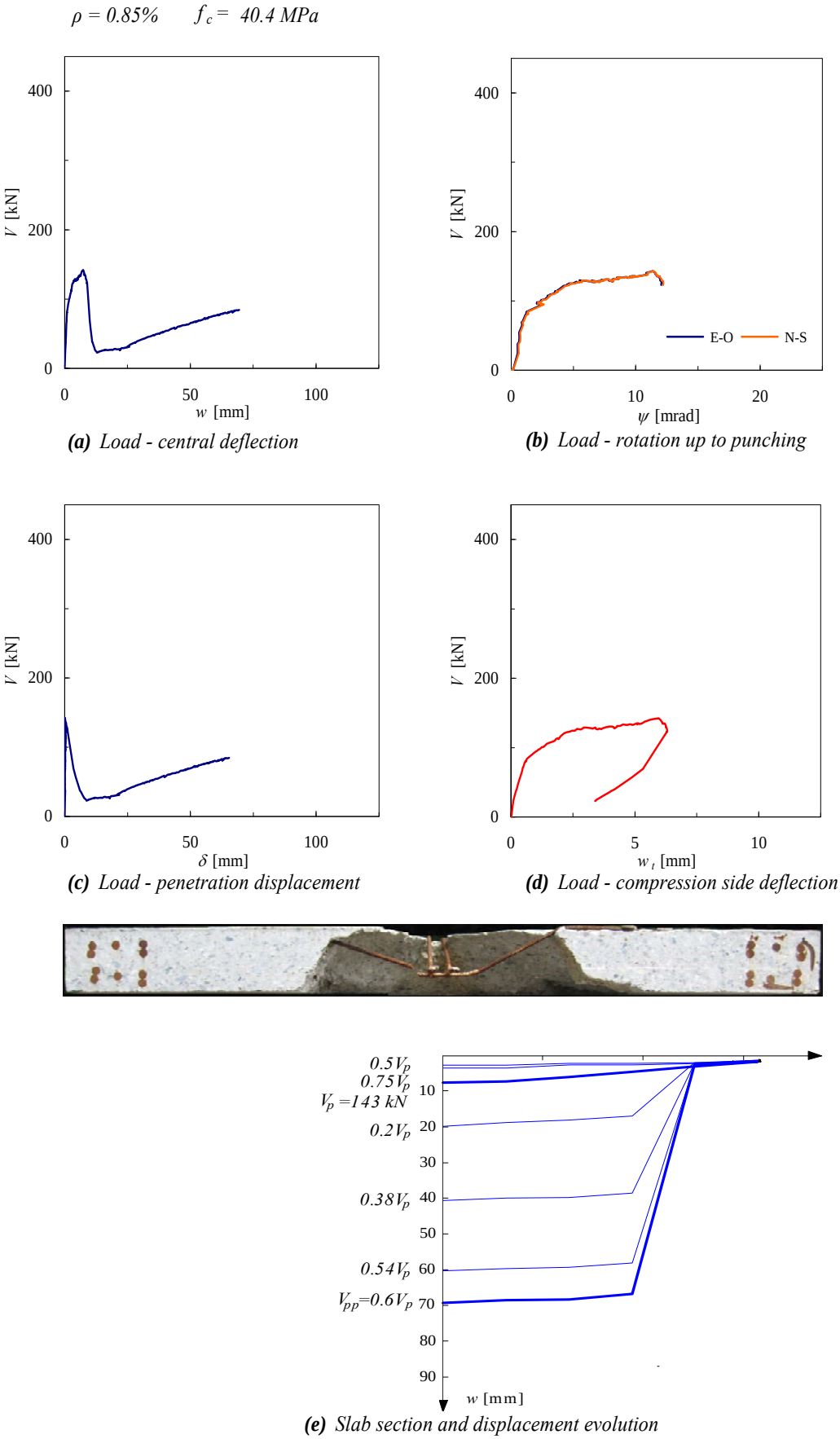

(a) *Load - central deflection*

(b) *Load - rotation up to punching*

(c) *Load - penetration displacement*

(d) *Load - compression side deflection*

(e) *Slab section and displacement evolution*

Figure 4.21: Slab PM-25: cut-off tensile reinforcement + compressive reinforcement Ø8

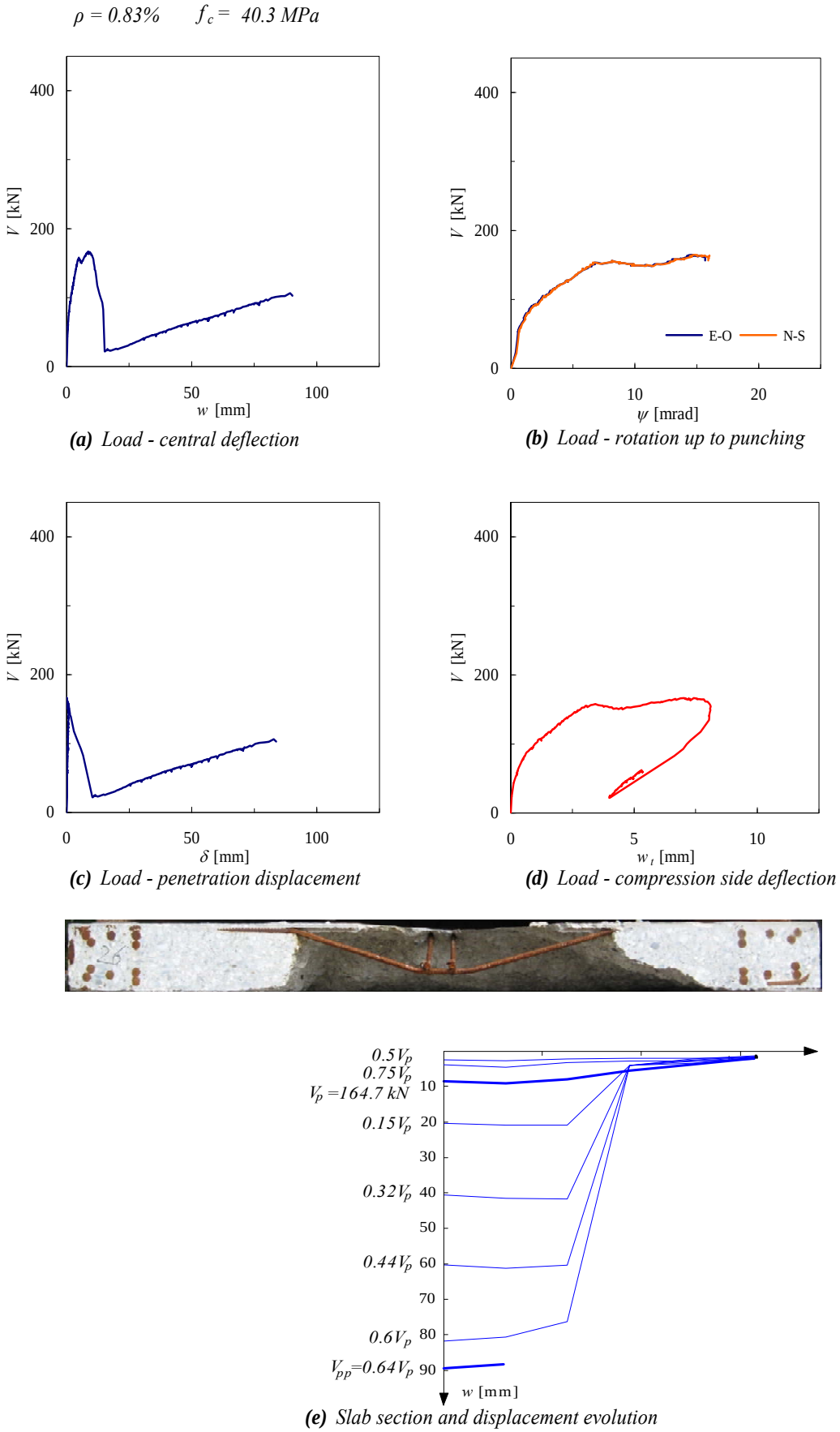

(a) *Load - central deflection*

(b) *Load - rotation up to punching*

(c) *Load - penetration displacement*

(d) *Load - compression side deflection*

(e) *Slab section and displacement evolution*

Figure 4.22: Slab PM-26: cut-off tensile reinforcement + compressive reinforcement Ø10

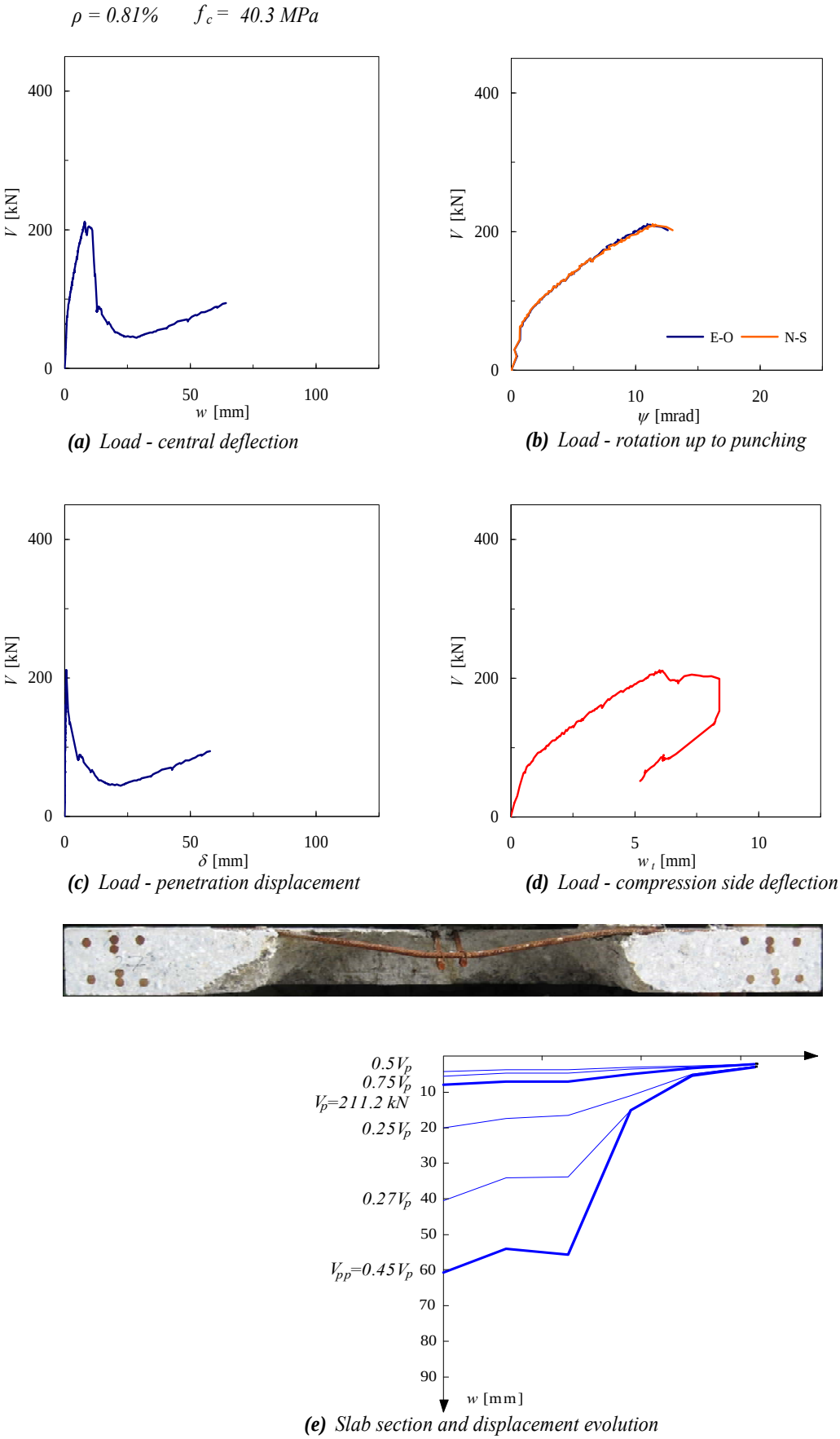

(a) *Load - central deflection*

(b) *Load - rotation up to punching*

(c) *Load - penetration displacement*

(d) *Load - compression side deflection*

(e) *Slab section and displacement evolution*

Figure 4.23: Slab PM-27: cut-off tensile reinforcement + compressive reinforcement Ø12

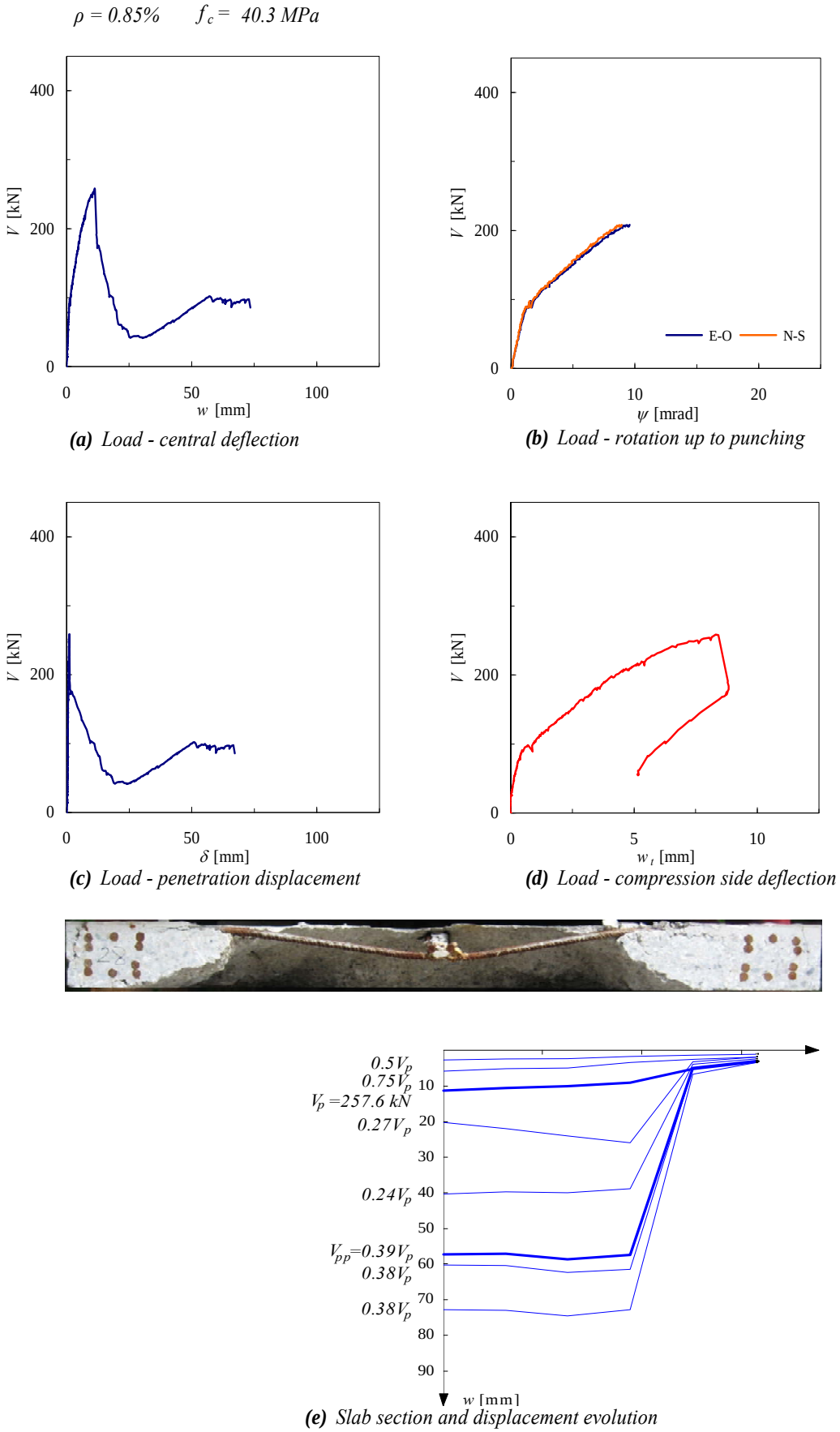

(a) *Load - central deflection*

(b) *Load - rotation up to punching*

(c) *Load - penetration displacement*

(d) *Load - compression side deflection*

(e) *Slab section and displacement evolution*

Figure 4.24: Slab PM-28: cut-off tensile reinforcement + compressive reinforcement Ø14

5 Summary of experimental results

The test results were compared to gain a better understanding of the influence of the different parameters on the post-punching behavior of flat slabs supported by columns. It was generally observed that after the punching shear strength has been reached, the load decreases rapidly. Then it starts increasing with further deflection. In all the specimens in the post-punching phase, the tensile reinforcement tend to tear out of concrete by a combination of bond failure and vertical tearing, especially in the vicinity of the column. At this stage, because of the large strains at the slab tension surface, cracks propagate through the slab and yielding of reinforcement spreads throughout the slab. The load is carried by the reinforcement acting as a tensile membrane and with further deflection, the load carried increases until the reinforcement starts to fracture.

PM-1 to PM-4: membrane effect

Fig. 5.1 shows the load-deflection responses of slabs PM-1 to PM-4, with the same geometry but different reinforcement ratios. As expected, the punching shear capacity increases as the reinforcement ratio increases. All specimens experienced punching shear failure and their post-punching behavior was observed. As can be seen in Fig. 5.1 the punching strength of PM-3 is slightly higher than that of PM-4. This difference in their response can be explained by the fact that the compressive strength of concrete at the time of testing was 39.5 MPa and 36.8 MPa for PM-3 and PM-4, respectively. It should also be mentioned that the punching shear strength of flat slabs is significantly influenced by the compressive strength of concrete; however in this case slab PM-4 had a larger reinforcement ratio. In this series of test, the only connection between truncated punching cone and the rest of the slab after punching failure was the tensile reinforcement. This connection made it possible for slabs to carry load after punching failure. The ratio of the maximum post-punching strength to the maximum punching strength was 0.21, 0.30, 0.36 and 0.37 for slabs PM-1, PM-2, PM-3 and PM-4, respectively. The relative small post-punching strength of these specimens was due to the fact that the tensile reinforcement almost completely spalled of concrete. Fig. 5.1 also shows the main results and mechanical properties of these specimens.

It should be noted that all experiments, PM-1 to PM-28, were terminated when the main measurement equipments were no longer able to record meaningful values due to the destruction of the punching cone.

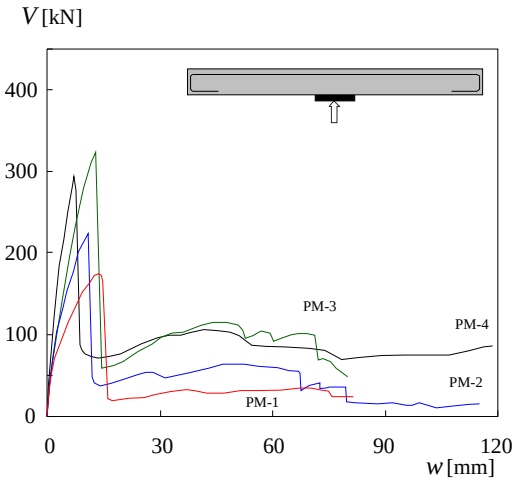

Test	f_c [MPa]	f_{syt} [MPa]	f_{syc} [MPa]	ρ [%]	A_{sb} -	V_p [kN]	w_p [mm]	V_{pp} [kN]
PM-1	36.6	601	-	0.82	-	175.8	13.6	37.2
PM-2	36.5	601	-	0.82	-	223.7	11.0	66.0
PM-3	37.8	601	-	0.82	-	324.3	13.1	117.4
PM-4	36.8	601	-	0.82	-	295.2	7.4	107.8

Figure 5.1: Load – deflection curve and main parameters for slabs PM-1 to PM-4

PM-9 to PM-12: straight compressive reinforcement for dowel action

Fig. 5.2 shows the load versus central deflection for slabs PM-9 to PM-12. Ø8, Ø10, Ø12 and Ø14 straight bar were used in the compression zone of these slabs. In this test series, the post-punching behavior was influenced not only by the tensile reinforcement but also by the compressive reinforcement. As load increases, cracks open, and interlocking of aggregate reduces quickly. Therefore, in the absence of shear reinforcement, the dowel action of longitudinal reinforcing bars plays a significant role in transferring shear when other contributions to the shear transfer are negligible as in the case of post-punching behavior of flat slabs. It can be observed that in these test specimens where the compressive reinforcing bars pass through the column, the post-punching load were clearly larger than that observed in the specimens without compressive reinforcement. The ratio of the maximum post-punching strength to the maximum punching strength was 0.55, 0.70, 0.98 and 0.98 for slabs PM-9, PM-10, PM-11 and PM-12, respectively. Although the punching strength was approximately the same for all specimens in this test series, there was a considerable difference in the post critical behavior of the first two specimens (PM-9 and PM-10), and the last two (PM-11 and PM-12). This can be attributed to the type of steel reinforcement. Cold worked steel was used for the former slabs, whereas hot rolled steel was used for the latter slabs. The sudden drops in the graphs are caused by the fracture of the steel bars.

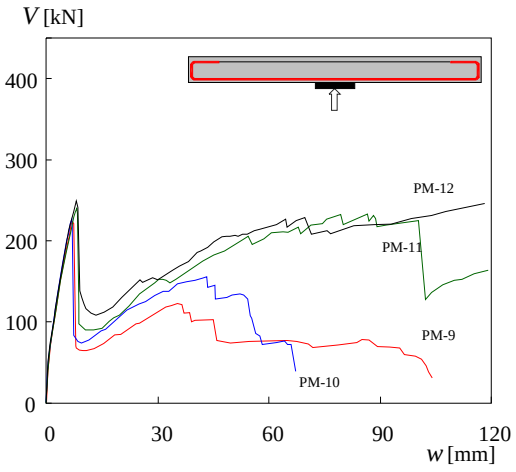

Test	f_c [MPa]	f_{syt} [MPa]	f_{syc} [MPa]	ρ [%]	A_{sb} -	V_p [kN]	w_p [mm]	V_{pp} [kN]
PM-9	31.0	601	616	0.82	4Ø8	224	7.1	123
PM-10	31.1	601	560	0.82	4Ø10	227	6.7	159
PM-11	32.3	601	548	0.82	4Ø12	241	8.2	236
PM-12	32.4	601	527	0.82	4Ø14	249	8.2	245

* cold – worked steel
** hot – rolled steel

Figure 5.2: Load – deflection curve and main parameters for slabs PM-9 to PM-12

PM-13 to PM-16: bent-up-bars, insufficient anchorage

Fig. 5.4 shows the load-deflection responses of slabs PM-13 to PM-16, each having the same geometry and tensile reinforcement but a different bent-up-bar diameter. All specimens experienced punching shear failure. As can be seen in Fig. 5.4, these test specimens have the same initial stiffness but their punching strengths are slightly different. As it pointed out earlier, the punching shear strength of flat slabs is significantly influenced by the compressive strength of concrete. According to Table 2.5 the compressive concrete strength for slabs PM-13 to PM-16 ranged from 30 to 34.5 MPa. This may partially explain the different punching strengths of these specimens. The ratio of the maximum post-punching strength to the maximum punching strength was 0.46, 0.53, 0.64 and 0.45 for slabs PM-13, PM-14, PM-15 and PM-16, respectively. The relative small post-punching strength of these specimens was due to the fact that the bent-up bars were not properly anchored as can occur in existing structures. According to the Swiss code SIA 262 the minimal anchorage length in the tension zone equals to forty times the bar diameter for the concrete type of C30/37 which is about 480 and 560 mm for Ø12 and Ø14, respectively. Fig. 5.3 shows the anchorage condition for the various integrity reinforcement as well as the possible cracking before punching failure. As it shown, there is no concern for compressive reinforcement crossing the column as well as for full-anchored bent-up bars (Fig. 5.3 a and c). However with the increase of the load and opening the punching cracks in the absence of the hook (Fig. 5.3 b), the bent-up bars experienced the bond failure thus losing their effectiveness. This can be attributed to the short anchorage length of 455 mm in combination with premature punching cracks along the bar.

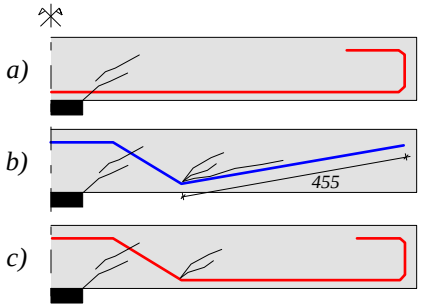

Figure 5.3: Anchorage condition for the various integrity reinforcement

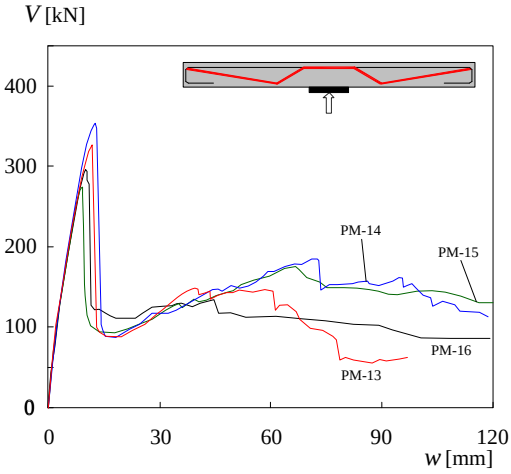

Test	f_c [MPa]	f_{syt} [MPa]	f_{syc} [MPa]	ρ [%]	A_{sb} -	V_p [kN]	w_p [mm]	V_{pp} [kN]
PM-13	32.6	601	616	0.82	4Ø8	327	11.4	151
PM-14	32.7	601	560	0.82	4Ø10	356	12.6	187
PM-15	32.7	601	548	0.84	4Ø12	274	9.1	177
PM-16	32.8	601	527	0.83	4Ø14	298	10.1	135

Figure 5.4: Load – deflection curve and main parameters for slabs PM-13 to PM-16

PM-17 to PM-20: fully anchored bent-up-bars

Fig. 5.5 shows the load-deflection responses for slabs PM-17 to PM-20. The bent-up bars which function as shear reinforcement were fully anchored. These specimens exhibited an improved punching behavior and larger post-punching strength. Detachment of the top reinforcement was observed. Compared to the other specimens, PM-19 and PM-20 exhibited a different behavior prior to the punching failure. The punching strength showed an increase of 28% and 23% to the respective experimental punching load for PM-19 and PM-20, respectively. They also experienced a very large deflection at punching failure showing a much more ductile behavior than the other specimens. The slab deflection at punching shear failure was 28.7 mm and 19.3 mm for PM-19 and PM-20, respectively.

The maximum loads obtained in the post-punching phase were clearly larger than those obtained in the slabs with compressive reinforcement passing through the column. The ratio of the maximum post-punching strength to the maximum punching strength was 0.75, 0.73, 0.75 and 0.86 for slabs PM-17, PM-18, PM-19 and PM-20, respectively. Although the ratio of the maximum post-punching strength to the punching shear strength for these two specimens were lower than those in slabs PM-11 and PM-12, the maximum post-punching load of PM-19 and PM-20 were 33% and 41% higher than those of slabs PM-11 and PM-12, respectively. These specimens showed that using bent-up bars passing through the column is probably more effective than compressive reinforcing bars in preventing the progressive collapse.

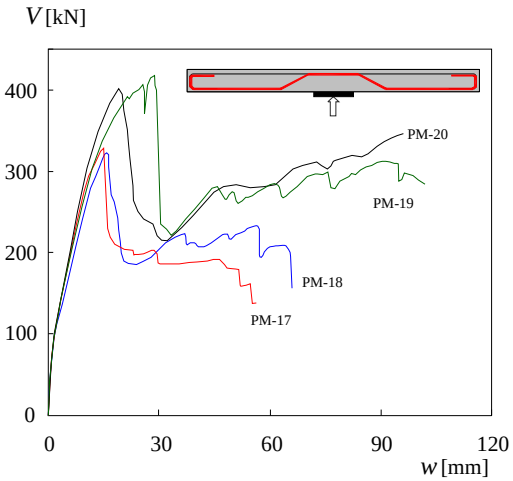

Test	f_c [MPa]	f_{syt} [MPa]	f_{syc} [MPa]	ρ [%]	A_{sb} -	V_p [kN]	w_p [mm]	V_{pp} [kN]
PM-17	39.7	625	625	0.82	4Ø8	329	15.1	247
PM-18	39.8	625	605	0.88	4Ø10	323	15.7	237
PM-19	39.9	625	559	0.85	4Ø12	417	28.7	315*
PM-20	40.0	625	578	0.82	4Ø14	402	19.3	345*

* Test terminated because the main measurement equipments were no longer able to record meaningful values

Figure 5.5: Load – deflection curve and main parameters for slabs PM-17 to PM-20

PM-21, PM-22: straight compressive reinforcement, hot-rolled steel

Fig. 5.6 shows the load-deflection responses of slabs PM-21, PM-22. These test specimens were similar to PM-9 and PM-10 respectively, however PM-22 had a different steel type. Cold worked steel had been used for PM-10 (ε_u = 6.2%) and hot-rolled steel was used for the slab specimen PM-22 (ε_u = 10.3%). The aim was to investigate the effect of the type and ductility of steel on the post-punching behavior. Using hot-rolled steel bars provided a better post-punching behavior and increased not only the punching strength but also the maximum post-punching strength and its corresponding displacement. The ratio of the maximum post-punching load to the maximum punching strength was 0.73 and 0.76 for slabs PM-21 and PM-22,

respectively. The concrete compressive strength for PM-9 and PM-10 was about 31 MPa and for PM-21 and PM-22 was about 40 MPa and thus the punching strength as well as the post-punching strength were influenced by the effect of the compressive strength of concrete (up to 15%).

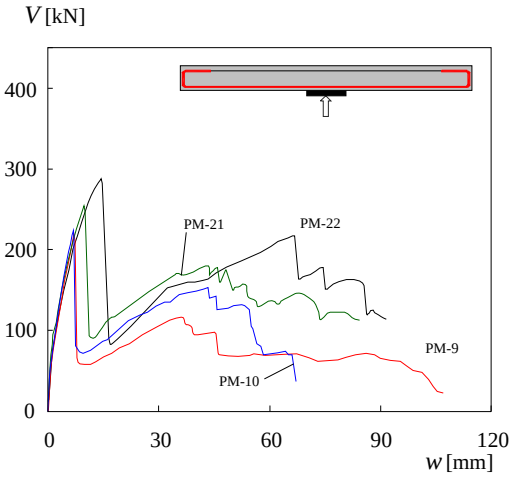

Test	f_c	f_{syt}	f_{syc}	ρ	A_{sb}	V_p	w_p	V_{pp}
PM-9	31.0	601	616*	0.82	4Ø8	224	7.1	123
PM-10	31.1	601	560*	0.82	4Ø10	227	6.7	159
PM-21	40.2	625	625*	0.81	4Ø8	256	9.7	185
PM-22	40.3	625	605**	0.85	4Ø10	288	14.1	219

* cold – worked steel
** hot – rolled steel

Figure 5.6: Load – deflection curve and main parameters for slabs PM-21,PM-22, PM-9 and PM-10

PM-23 and PM-24: membrane effect and confinement reinforcement

Fig. 5.7 shows the load versus central deflection for slabs PM-23 and PM-24. These specimens were geometrically similar and hence the punching and the post-punching behavior of them were nearly the same. No additional reinforcement was used and thus the membrane effect was the only factor influencing the post-punching response. The ratio of the maximum post-punching strength to the maximum punching strength was 0.36 and 0.37 for slabs PM-23 and PM-24, respectively. Slab PM-23 was the reference slab and thus only tensile reinforcement was used, whereas for slab PM-24 some stirrups were also placed above the column to investigate the effect of confinement reinforcement on the punching and post-punching behavior. As can be seen in Fig. 5.7, using confinement reinforcement above the column increased slightly the punching strength as well as the post-punching strength.

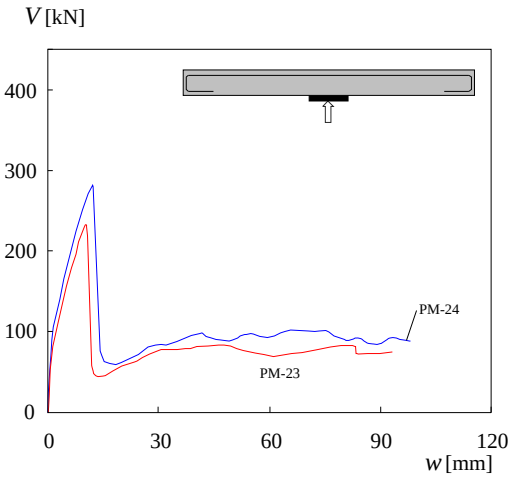

Test	f_c [MPa]	f_{syt} [MPa]	f_{syc} [MPa]	ρ [%]	A_{sb} -	V_p [kN]	w_p [mm]	V_{pp} [kN]
PM-23	40.4	625	-	0.81	-	227	10.4	82
PM-24	40.4	625	-	0.85	-	272	12.1	101

Figure 5.7: Load – deflection curve and main parameters for slabs PM-23 and PM-24

PM-25 to PM-28: cut-off tensile reinforcement + compressive reinforcement

Fig. 5.8 shows the load-deflection responses for slabs PM-25 to PM-28. In this test series, tensile reinforcing bars were cut off at the specified points, to specifically investigate the effect of the compressive reinforcement on the post-punching behavior. Cutting-off the tensile reinforcing bars localized the punching cracks at the end of the bars and as a result, the tensile reinforcing bars were not activated after punching failure. Therefore, the only factor affecting the post-punching response in these specimens was the dowel action due to the straight compressive reinforcement. The ratio of the maximum post-punching strength to the maximum punching strength was 0.60, 0.64, 0.45 and 0.39 for slabs PM-25, PM-26, PM-27 and PM-28, respectively. It was observed that using improper anchored tensile reinforcement (cut-off of tensile reinforcement) significantly reduced the punching strength, the post-punching strength and also the ductility of the slab-column connection. These specimens provided the opportunity of studying the effect of compressive reinforcement passing through the column. However, due to the fact that the only connection between the punching cone and the rest of slab was a small portion of the compressive reinforcing bars over the column, the risk of falling down the punching cone and other technical problems the tests were stopped before the specimens reached to their maximum post-punching strength. In addition, the punching cone was completely separated of the slab at the end of these experiments.

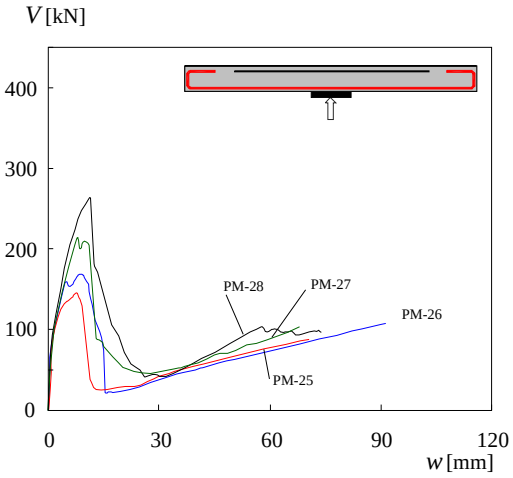

Test	f_c [MPa]	f_{svt} [MPa]	f_{svc} [MPa]	ρ [%]	A_{sb} -	V_p [kN]	w_p [mm]	V_{pp} [kN]
PM-25	40.4	625	625	0.85	4Ø8	143	7.7	85
PM-26	40.3	625	605	0.83	4Ø10	165	8.5	105
PM-27	40.3	625	559	0.81	4Ø12	211	8	94
PM-28	40.3	625	578	0.85	4Ø14	258	11.2	101

Figure 5.8: Load – deflection curve and main parameters for slabs PM-25 to PM-28

6 References

1. SIA, *SIA 262:2003, Construction en béton*, Société Suisse des Ingénieurs et des Architectes, Norme suisse SN 505 262, Switzerland, French, 2003.
2. MUTTONI A., FERNÁNDEZ RUIZ M., *Shear strength of members without transverse reinforcement as function of critical shear crack width*, ACI Structural Journal, V. 105, No 2, pp. 163-172, Farmington Hills, USA, 2008.
3. MUTTONI A., *Punching shear strength of reinforced concrete slabs without transverse reinforcement*, ACI Structural Journal, V. 105, N° 4, pp. 440-450, USA, 2008.
4. MUTTONI A., GUANDALINI S., FERNÁNDEZ RUIZ M., *Comportement mécanique des dalles et planchers-dalles en béton armé*, Documentation SIA, D 0226 : Sécurité structurale des parkings couverts, pp. 13-28, Zürich, Switzerland, French, 2008.
5. MUTTONI A., FERNÁNDEZ RUIZ M., *Shear strength in one- and two-way slabs according to the critical shear crack theory*, fib Symposium, Amsterdam 2008, Amsterdam, Netherlands, 2008.
6. BROMS C. E., *Elimination of Flat Plate Punching Failure Mode*, ACI Structural Journal, V. 97, No. 1, p. 94 - 101, 2000.
7. CSA STANDARD A23.3-04, *Canadian Standard Association*, 232 p, 2004.
8. ACI, Building Code Requirements for Structural Concrete, ACI American Concrete Institute, ACI 318-05, 430 p., USA, 2005.
9. ACI 352.1R-89, Recommendations for Design of Slab-Column Connections in Monolithic Reinforced Concrete (Reapproved 1997), ACI American Concrete Institute, 22 p., USA, 1997.
10. DIN, *DIN 1045-1 Tragwerke aus Beton und Stahlbeton*, DIN 1045-1, Deutsches Institut für Normung, 2nd Edition, 148 p., Berlin, Germany, German, 2005.
11. EUROCODE , *Eurocode 2: Design of concrete structures - Part 1-1: General rules and rules for buildings*, European Committee for Standardization (CEN), Brussels, 2004.
12. BS 8110-97, Structural use of concrete: Part 1: Code of practice for design and construction, British Standard Institute, London, p.117.
13. VAZ RODRIGUES R., *Shear Strength of Reinforced Concrete Bridge Deck Slabs*, EPFL, PhD thesis, n° 3739, 289 p., Lausanne, Switzerland, 2007.
14. CEB, CEB-FIP Model Code 1990, *Bulletin d'information No. 213/214*, may, 1993.

A Comparison of post-punching provisions in various codes

Generally the design of reinforced concrete flat slabs is governed by punching shear strength. Many tests have been done in the past to gain a better understanding of the behavior of flat slabs; however the current codes of practice differ significantly. Consequently, the calculation of the punching or post-punching strength and the relevant detailing of reinforcement depend considerably on the code applied. Therefore, the reinforcement layout might be very different in different countries.

Experience has shown that the overall integrity of a structure can be significantly enhanced by minor changes in reinforcement detailing. The tendency of the codes of practice is to increase the redundancy and ductility in structures so that in the event of damage to a major supporting element or an abnormal loading event, the resulting damage may be confined to a relatively small area. Therefore the structure will have a better chance to maintain overall stability. Redistribution of loads following a local damage to a structure depends on strength, continuity, redundancy, and deformation and energy dissipation capacities of the structure; however, in the case of punching failure, the drop in resistance can be large and can thus trigger failure at adjacent columns and lead to the progressive collapse of a large part of the structure. Alternate load path, dowel bars, integrity provisions and specific load resistance are means of providing redundancy or continuity to mitigate possible progressive collapse. When punching failure occurs, top reinforcement that is continuous over the support, but not confined by stirrups in the case of flat slabs without shear reinforcement, will tend to tear out of concrete and will not provide the catenary action needed to connect the damaged parts of structure. By making a portion of compressive reinforcement continuous, the overall stability could be obtained and the likelihood of that a local punching failure could lead to progressive collapse is reduced.

A.1 Swiss concrete code SIA 262 (2003)

To prevent the slab from totally collapsing after a possible punching, the Swiss code [1] requires that some reinforcement shall be provided on the flexural compression side. The reinforcement shall be extended over the supported area and dimensioned as follows:

$$V_d = A_{sb} \cdot f_{sd} \cdot \sin \beta \tag{A.1}$$

Assuming $\beta = 42°$ leads to:

$$A_{sb} > 1.5 \frac{V_d}{f_{sd}} \tag{A.2}$$

Where A_{sb} is the cross-sectional area of the reinforcing steel bars crossing the truncated punching cone, f_{sd} is the yield strength of the reinforcing steel, V_d is the dimensioning value of punching force and β is the angle of inclination of the reinforcing steel bars in the vicinity of the punching shear crack after failure as shown in Fig. A.1.

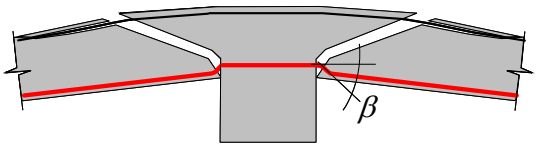

Figure A.1: Punching failure of concrete flat slab

A.2 Canadian code CSA A23.3-04 (2004)

CSA [7] requires that the summation of the area of compression reinforcement connecting the slab, drop panel, or slab band to the column or column capital on all faces of the periphery of the column or column capital shall be

$$\sum A_{sb} > 2\frac{V_{se}}{f_y} \tag{A.3}$$

where V_{se} is shear force transmitted to column or column capital due to specified loads. Table A.1 presents a summary of comparison between test results and the Swiss and Canadian codes of practice. According to the CSA A23 Clause 13.2.1 the minimum slab thickness shall be based on serviceability requirements but shall be not less than 120 mm and as a result the slab thickness of 125 mm, PM-1 to PM-28, is satisfactory.

Table A.1: Summary of comparison between the test results and the Swiss and Canadian codes

Test	ρ [%]	A_{sb}	$V_{p,test}$ [kN]	$V_{pp,test}$ [kN]	V_{SIA} [kN]	V_{CSA} [kN]	$\frac{V_{pp,test}}{V_{SIA}}$	$\frac{V_{pp,test}}{V_{CSA}}$
PM-1	0.25%	-	175.8	37.2	0	0	-	-
PM-2	0.49%	-	223.7	66	0	0	-	-
PM-3	0.82%	-	324.3	117.4	0	0	-	-
PM-4	1.41%	-	295.2	107.8	0	0	-	-
PM-9	0.82%	4Ø8	224.2	123.4	129.9	121	0.95	1.02
PM-10	0.82%	4Ø10	227.5	158.6	189.6	176	0.84	0.90
PM-11	0.82%	4Ø12	240.6	236.5	266.3	248	0.89	0.96
PM-12	0.82%	4Ø14	249	245	348.6	324	0.71	0.76
PM-13	0.82%	4Ø8	326.7	150.6	129.9	121	1.15	1.25
PM-14	0.82%	4Ø10	355.8	187.5	189.6	176	0.99	1.07
PM-15	0.82%	4Ø12	274	176.7	266.3	248	0.67	0.71
PM-16	0.82%	4Ø14	298.4	134.8	348.6	324	0.38	0.42
PM-17	0.82%	4Ø8	329.1	246.6	135.6	126	1.82	1.96
PM-18	0.82%	4Ø10	322.7	236.7	205.0	190	1.15	1.24
PM-19	0.82%	4Ø12	417.3	315	275.2	256	1.14	1.23
PM-20	0.82%	4Ø14	402.1	344.9	382.5	356	0.90	0.97
PM-21	0.82%	4Ø8	255.7	185.4	135.6	126	1.38	1.48
PM-22	0.82%	4Ø10	288.2	218.7	205.0	190	1.07	1.15
PM-23	0.82%	-	227	82.2	0.0	0	-	-
PM-24	0.82%	-	271.5	100.6	0.0	0	-	-
PM-25	0.82%	4Ø8	143	85.4	135.6	126	0.63	0.68
PM-26	0.82%	4Ø10	164.7	104.6	205.0	190	0.51	0.55
PM-27	0.82%	4Ø12	211.2	94.1	275.2	256	0.35	0.37
PM-28	0.82%	4Ø14	257.6	101.4	382.5	356	0.26	0.29
					average		0.88	0.95
					standard deviation		0.39	0.41

A.3 American code ACI 318-05 (2005)

ACI 318 [8] has no explicit formula for post-punching behavior of concrete flat slabs and only proposes some requirements for structural integrity. The code requires that all bottom bars within the column strip be continuous. At least two compressive reinforcing bars in each direction shall pass through the column core and shall be anchored at exterior supports. The two continuous compressive bars passing through the column may be termed integrity steel, and are provided to give the slab some residual capacity to prevent a local failure over a column lead to the progressive collapse of a large part of the structure.

Although ACI 318 does not explicitly deal with the phenomenon of the progressive collapse ACI 352.1R-89 [9] proposed some recommendations to reduce the likelihood of this phenomenon. ACI 352.1R-89 recommends that at interior connections, continuous bottom reinforcement passing within the column cage in each principal direction should have an area at least equal to

$$A_{sb} = \frac{0.5 q_d \ell_1 \ell_2}{\Phi f_y} \tag{A.4}$$

in which A_{sb} = minimum area of effectively continuous bottom bars or mesh in each principal direction placed over the support, q_d = factored uniformly distributed load, but not less than twice the slab service dead load, ℓ_1 and ℓ_2 = center-to-center span in each principal direction, f_y = yield stress of steel A_{sb}, and Φ = 0.9. The quantity of reinforcement A_{sb} may be reduced to two thirds of that given quantity for edge connections, and to one-half of that for corner connections.

A.4 DIN 1045-1

DIN 1041-1 [10] specifies the following formula to estimate the area of compression reinforcement passing thorough the column and properly anchored in the slab to mitigate the likelihood of the progressive collapse phenomenon:

$$A_{sb} = \frac{V_{Ed}}{f_{yk}} \tag{A.5}$$

where V_{Ed} is the design value of the punching force and f_{yk} is the characteristic value of the cylinder compressive strength.

A.5 European standard Eurocode 2 (2004)

Eurocode 04-2 [11] is a model code adopted by many European countries that may also supplement it with national standards. Eurocode has no explicit requirement for post-punching behavior of concrete flat slabs. It merely recommends that at least two bottom reinforcement bars in each orthogonal direction should be provided at internal columns and this reinforcement should pass through the column. In addition to providing general design guidelines to avoid progressive collapse, such as selection of a good structural layout, Eurocode also recommends tying the building together and defines values for tie forces.

A.6 British Standards

Although British code [12] does not directly deal with the post-punching behavior of flat slabs, it provides some recommendation to mitigate the risk of progressive collapse due to a local failure. British Standards emphasize general tying of various structural elements of a building together, to provide continuity and redundancy. Ties enhance the resistance of wall panels to being blown away in the event of a failure, and also the ability of a structure to bridge over a lost support.

B Failure criterion (Muttoni 2003)

Muttoni et al. [2-5] proposed a failure criterion for the symmetric punching of reinforced concrete flat slabs without shear reinforcement which can determine the punching strength mainly as a function of the radial rotation of the slab in the vicinity of the slab-column connection. The shear strength can be expressed as a function of the deformation in the critical region as indicated by this equation:

$$\tau_R = \frac{\tau_c}{0.4 + 0.125 \cdot \psi \cdot d \cdot k_{D\max}} \tag{B.1}$$

where ψ is the rotation of the slab, d is the effective depth of the slab and $\tau_c = 0.3\sqrt{f_c}$ is the nominal shear strength of concrete. The effect of the maximum aggregate size D_{max} [mm] is takes into account by $k_{D\max} = 48/(D_{\max} + 16)$. The term of $\tau_R = \frac{V_p}{u \cdot d}$ is the punching shear resistance, where V_p is the maximum punching shear force and u is the length of the control perimeter according to the Swiss code SIA 262 (2003).

Figure B.1 shows the comparison of the proposed failure criterion with the punching shear tests carried out in this experimental program. It can be observed that there is a very good agreement between test results and the failure criterion for slabs without shear reinforcement. Slabs PM-13 to PM-20 include bent-up bars acting as shear reinforcement. Therefore, the proposed rotation-based failure criterion for slabs without shear reinforcement is not applicable. As pointed out before, slabs PM-25 to PM-28 had cut-off tensile reinforcement and consequently their punching strength decreased significantly as can be seen in Fig. B.1e.

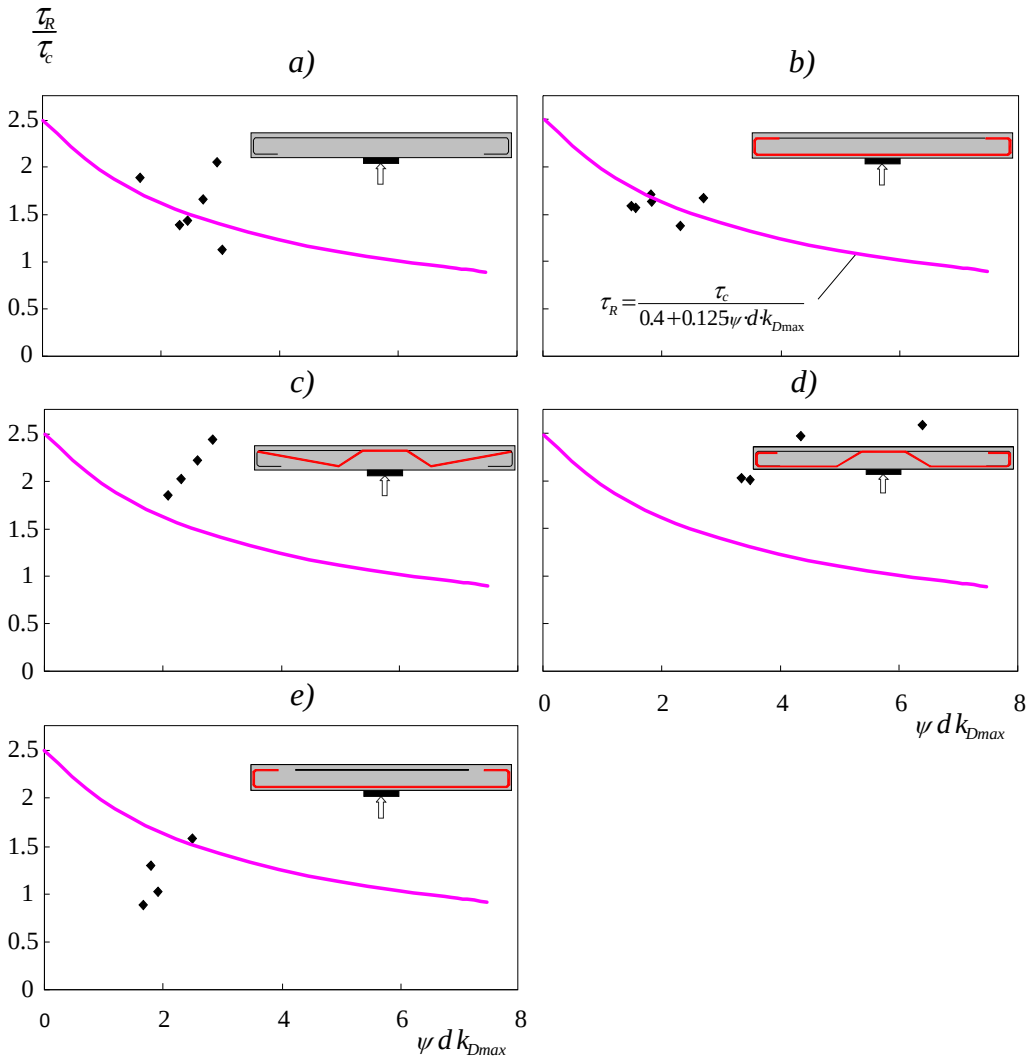

Figure B.1: Comparison of punching shear test results with the failure criterion: a) PM-1 to PM-4, PM-23 and PM-24 b) PM-9 to PM-12, PM-21 and PM-22 c) PM-13 to PM-16 d) PM-17 to PM-20 e) PM-25 to PM-28

C Summary of experimental results

	Test	age	f_c	f_{ct}	E_c	d	ρ	*Tensile reinf.*				A_{sb}	*Integrity reinf.*				V_p	w_p	V_{pp}	w_{pp}	$\frac{V_{pp}}{V_p}$	*Reinforcement layout*	A_s	A_{sb}	Test
		[day]	[MPa]	[MPa]	[GPa]	[mm]	[%]	f_{sy} [MPa]	f_{su} [MPa]	ε_{su} [%]	E_s [GPa]		f_{sy} [MPa]	f_{su} [MPa]	ε_{su} [%]	E_s [GPa]	[kN]	[mm]	[kN]	[mm]					
Series 1	PM-1	33	36.6	2.9	36.9	102	0.25	601	664	7.4	201	-	-	-	-	-	176	13.6	37	70.5	0.21	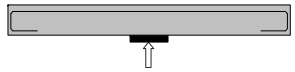	Ø8@200	-	PM-1
	PM-2	30	36.5	2.8	36.7	102	0.49	601	664	7.4	201	-	-	-	-	-	224	11.0	66	52.7	0.30		Ø8@100	-	PM-2
	PM-3	71	37.8	3.4	37.9	102	0.82	601	664	7.4	201	-	-	-	-	-	324	13.1	117	45.3	0.36		Ø8@60	-	PM-3
	PM-4	38	36.8	3.0	37.1	102	1.41	601	664	7.4	201	-	-	-	-	-	295	7.4	108	42.6	0.37		Ø8@35	-	PM-4
Series 2	PM-9	35	31.0	2.3	33.3	102	0.82	601	664	7.4	201	4Ø8	616	680	7.4	202	224	7.1	123	36.2	0.55	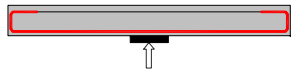	Ø8@60	4Ø8	PM-9
	PM-10	37	31.1	2.3	33.3	102	0.82	601	664	7.4	201	4Ø10	560	599	7.9	195	228	6.7	159	42.9	0.70		Ø8@60	4Ø10	PM-10
	PM-11	56	32.3	2.5	33.7	102	0.82	601	664	7.4	201	4Ø12	548	625	10.5	201	241	8.2	237	86.3	0.98		Ø8@60	4Ø12	PM-11
	PM-12	58	32.4	2.6	33.7	102	0.82	601	664	7.4	201	4Ø14	527	629	13.5	199	249	8.2	245	116.9	0.98		Ø8@60	4Ø14	PM-12
	PM-13*	62	32.6	2.6	33.8	102	0.82	601	664	7.4	201	4Ø8	616	680	7.4	202	327	11.4	151	39.9	0.46	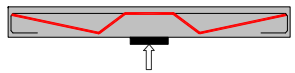	Ø8@60	4Ø8	PM-13
	PM-14*	64	32.7	2.6	33.8	102	0.82	601	664	7.4	201	4Ø10	560	599	7.9	195	356	12.6	188	71.7	0.53		Ø8@60	4Ø10	PM-14
	PM-15*	65	32.7	2.6	33.8	100	0.84	601	664	7.4	201	4Ø12	548	625	10.5	201	274	9.1	177	66.5	0.64		Ø8@60	4Ø12	PM-15
	PM-16*	68	32.8	2.6	33.9	101	0.83	601	664	7.4	201	4Ø14	527	629	13.5	199	298	10.1	135	43.4	0.45		Ø8@60	4Ø14	PM-16
Series 3	PM-17	35	39.7	2.8	28.7	102	0.82	625	641	6.1	200	4Ø8	625	641	6.1	200	329	15.1	204	50.0	0.75	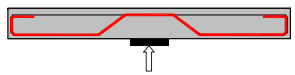	Ø8@60	4Ø8	PM-17
	PM-18	36	39.8	2.8	28.8	95	0.88	625	641	6.1	200	4Ø10	605	658	7.8	194	323	15.7	237	56.5	0.73		Ø8@60	4Ø10	PM-18
	PM-19	37	39.9	2.8	28.8	99	0.85	625	641	6.1	200	4Ø12	559	618	7.9	197	417	28.7	315	90.1	0.75		Ø8@60	4Ø12	PM-19
	PM-20	39	40.0	2.9	29.0	102	0.82	625	641	6.1	200	4Ø14	578	695	12.0	203	402	19.3	345	95.2	0.86		Ø8@60	4Ø14	PM-20
	PM-21	43	40.2	2.9	29.3	103	0.81	625	641	6.1	200	4Ø8	625	641	8.9	200	256	9.7	185	42.9	0.73	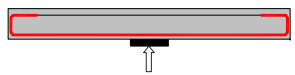	Ø8@60	4Ø8	PM-21
	PM-22	46	40.3	2.9	29.5	99	0.85	625	641	6.1	200	4Ø10	605	658	10.3	194	288	14.1	219	65.2	0.76		Ø8@60	4Ø10	PM-22
	PM-23	50	40.4	2.9	29.7	95	0.88	625	641	6.1	200	-	-	-	-	-	227	10.4	82	83.0	0.36		Ø8@60	-	PM-23
	PM-24	53	40.4	3.0	29.9	97	0.86	625	641	6.1	200	-	-	-	-	-	272	12.1	101	74.2	0.37		Ø8@60	-	PM-24
	PM-25$^+$	56	40.4	3.0	30.1	98	0.85	625	641	6.1	200	4Ø8	625	641	6.1	200	143	7.7	85	69.8	0.60	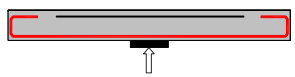	Ø8@60	4Ø8	PM-25
	PM-26$^+$	57	40.3	3.0	30.1	101	0.83	625	641	6.1	200	4Ø10	605	658	7.8	194	165	8.5	105	89.3	0.64		Ø8@60	4Ø10	PM-26
	PM-27$^+$	58	40.3	3.0	30.2	104	0.81	625	641	6.1	200	4Ø12	559	618	7.9	197	211	8.0	94	64.1	0.45		Ø8@60	4Ø12	PM-27
	PM-28$^+$	60	40.3	3.0	30.3	99	0.85	625	641	6.1	200	4Ø14	578	695	12.0	203	258	11.2	101	57.2	0.39		Ø8@60	4Ø14	PM-28

+ : Test deliberately terminated due to the risk of falling down the punching cone
* : Anchorage failure

D Notations

A_{sb}	Area of the compressive reinforcement bars passing through the column
A_s , A_{st}	Area of tensile reinforcement
B	Slab width
E_s	Modulus of elasticity of steel reinforcement
E_c	Modules of elasticity of concrete
D_{max}	Maximum aggregate size
V_{se}	Shear force transmitted to column
V_d, V_{Ed}	Dimensioning value of punching force
V_p, $V_{p,test}$	Maximum load at the punching failure
V_{pp}, $V_{pp,test}$	Maximum load after the punching failure
V_{SIA}	Post punching strength calculated according to the SIA 262
V_{CSA}	Post punching strength calculated according to the CSA A-23
a	Column width
age	Age of specimen at time of testing
d	Effective depth of reinforced concrete flat slab
k_{Dmax}	Coefficient taking into account the maximum aggregate size
ℓ	Length of rebar measured between the clamps of the tension testing machine
ℓ_b	Anchorage length
ℓ_1, ℓ_2	Center-to-center span in each principal direction
f_{yk}	Characteristic value of yield strength of reinforcing steel
f_{sd}	Design yield strength of steel reinforcement
f_{sv} , f_y	Yielding strength of reinforcement
f_{svc}	Yielding strength of the compressive reinforcement or integrity reinforcement
f_{syt}	Yielding strength of the tensile reinforcement
f_t	Ultimate tensile strength of steel reinforcement
f_{tc}	Ultimate tensile strength of the compressive reinforcement or integrity reinforcement
f_{tt}	Ultimate tensile strength of the tensile reinforcement
f_c	Compressive strength of concrete
$f_{c,28}$	Cylinder compressive strength at the age of 28 days
f_{ct}	Tensile strength of concrete
h	Slab thickness
q_d	Factored uniform load
u	Length of the control perimeter
w	Slab deflection
w_t	Average deflection of slab compression side at the distance of 240 mm from the center
w_p, $w_{p,test}$	Deflection corresponding to the maximum load at the punching failure
w_{pp},	Deflection corresponding to the maximum load after the punching failure
α	Angle of inclination of the punching cone

β	Angle of inclination of compressive reinforcement after failure
δ	Relative penetration displacement
Φ	Strength reduction factor
ψ	Slab rotation
σ_c	Compressive stress of concrete
ρ	Tensile reinforcement ratio
Ø	Diameter of reinforcing bar
ϕ_t	Diameter of tensile reinforcing bar
ϕ_c	Diameter of compressive reinforcing bar, bent-up bar diameter
τ	Shear stress
τ_c	Nominal shear stress of concrete
τ_R	Punching shear stress
ε	Strain
ε_c	Compressive strain of concrete
ε_s	Strain in reinforcement steel
ε_y	Yielding strain of steel reinforcement
ε_u	Ultimate strain of steel reinforcement